Published in final edited form as:
Hippocampus. 2009 April ; 19(4): 321–337. doi:10.1002/hipo.20516.

A Role for Hilar Cells in Pattern Separation in the Dentate Gyrus: A Computational Approach

Catherine E. Myers[1,*] and **Helen E. Scharfman**[2,3,4]

[1]Department of Psychology, Rutgers University-Newark, Newark, New Jersey

[2]Department of Child and Adolescent Psychiatry, New York University School of Medicine, New York, New York

[3]Department of Physiology and Neuroscience, New York University School of Medicine, New York, New York

[4]Center for Dementia Research, The Nathan Kline Institute for Psychiatric Research, Orangeburg, New York

Abstract

We present a simple computational model of the dentate gyrus to evaluate the hypothesis that pattern separation, defined as the ability to transform a set of similar input patterns into a less-similar set of output patterns, is dynamically regulated by hilar neurons. Prior models of the dentate gyrus have generally fallen into two categories: simplified models that have focused on a single granule cell layer and its ability to perform pattern separation, and large-scale and biophysically realistic models of dentate gyrus, which include hilar cells, but which have not specifically addressed pattern separation. The present model begins to bridge this gap. The model includes two of the major subtypes of hilar cells: excitatory hilar mossy cells and inhibitory hilar interneurons that receive input from and project to the perforant path terminal zone (HIPP cells). In the model, mossy cells and HIPP cells provide a mechanism for dynamic regulation of pattern separation, allowing the system to upregulate and downregulate pattern separation in response to environmental and task demands. Specifically, pattern separation in the model can be strongly decreased by decreasing mossy cell function and/or by increasing HIPP cell function; pattern separation can be increased by the opposite manipulations. We propose that hilar cells may similarly mediate dynamic regulation of pattern separation in the dentate gyrus in vivo, not only because of their connectivity within the dentate gyrus, but also because of their modulation by brainstem inputs and by the axons that "backproject" from area CA3 pyramidal cells.

Keywords

hippocampus; dentate gyrus; computational model; hilus; pattern separation

INTRODUCTION

The mammalian hippocampus, including area CA1 and CA3 as well as the dentate gyrus, has long been acknowledged to play a key role in learning and memory, both in laboratory animals and in humans (Squire, 1992; Cohen and Eichenbaum, 1993; Gluck and Myers, 2001;

*Correspondence to: Catherine E. Myers, Memory Disorders Project, Rutgers-Newark, 197 University Avenue, Suite 209, Newark, NJ 07102, USA. E-mail: myers@pavlov.rutgers.edu.

Eichenbaum, 2002; Andersen et al., 2006; Scharfman, 2007a). Hippocampal field CA3 has often been suggested to function as a content-addressable memory, meaning that it is capable of performing pattern storage and also of reconstructing stored patterns from incomplete inputs, a process known as pattern completion; this idea of the hippocampal region as a content-addressable memory dates back at least to David Marr (Marr, 1971) and was later elaborated by many others including Rolls (1989a,b, 1996, 2007), McNaughton and Morris (McNaughton and Morris, 1987; McNaughton, 1991), and Levy (1985).

The storage capacity of such of a content-addressable memory, in terms of the number of patterns that can be stored and retrieved, is highest if the patterns to be stored do not overlap extensively (Marr, 1971; Willshaw and Buckingham, 1990); in this context, overlap is defined as the degree to which individual elements that are active or inactive in one pattern are also active or inactive in another pattern. The capacity of a content-addressable memory can therefore be increased by transforming the to-be-stored patterns so that overlap is reduced between them, a process termed pattern separation. Pattern separation can be achieved in two basic ways. First, the patterns themselves can be made sparser, meaning that fewer elements are active within a pattern; second, the particular elements that are active in each pattern can be orthogonalized, meaning that a different subset of elements is active in each of the patterns (Rolls, 1989a,b; O'Reilly and McClelland, 1994).

Given the premise that CA3 performs pattern storage and pattern completion, and that this function could be optimized by a preprocessor that performs pattern separation, it was perhaps natural to look to the dentate gyrus, which is commonly viewed as a primary waystation for entorhinal inputs traveling to CA3 (but see, Yeckel and Berger, 1990; Derrick, 2007). Rolls, in particular, suggested that several features of the dentate gyrus contribute to produce pattern separation, including the low firing probability of dentate granule cells and the low contact probability of dentate granule cell axons to CA3 pyramidal cells; both features could decrease the probability that two separate entorhinal input patterns activate the same subset of CA3 neurons (Rolls, 1989a,b).

Empirical data have also accumulated to show that the dentate gyrus is not merely a "passive" waystation for information traveling into the hippocampus, but rather shows learning-related changes (e.g., Hampson and Deadwyler, 1992); age-related decline in these processes may be an important component of the cognitive impairments observed in aging (Chawla and Barnes, 2007). Rolls et al. suggested that learning-related changes in the dentate gyrus could further improve pattern separation, specifically through a process of "competitive learning" in the dentate gyrus, meaning that activated granule cells excite interneurons that inhibit other granule cells, and only those "winning" granule cells that "survive" inhibition undergo synaptic plasticity, making them more likely to respond to similar inputs in the future and therefore "win" the competition (Rolls, 1989b). Rolls et al. have implemented these ideas in an elegant series of computational models of the hippocampus, and have showed that these models can successfully perform pattern storage and completion, and account for a range of empirical data (Rolls, 1989a,b, 1996, 2007; Treves and Rolls, 1992, 1994; Rolls and Kesner, 2006; Rolls et al., 2006). Other models of hippocampal function have also incorporated variations on the basic ideas of CA3 as a content-addressable memory store and of the dentate gyrus as a preprocessor performing pattern separation on entorhinal inputs to CA3 (e.g., McNaughton and Morris, 1987; Levy, 1990; O'Reilly and McClelland, 1994; McClelland and Goddard, 1996; Norman and O'Reilly, 2003; Meeter et al., 2004), and the basic ideas originally espoused by Marr, Rolls, and their colleagues have generally been validated by subsequent studies of dentate and hippocampal anatomy and physiology (see Rolls and Kesner, 2006; Acsády and Káli, 2007; Kesner, 2007).

A newer generation of computational models has taken this basic premise further, to incorporate the implications of postnatal neurogenesis of granule cells in the dentate gyrus (for review, see Kempermann, 2006). The recent models have suggested that addition of newly born neurons to a network can increase storage capacity, while avoiding storage problems that can occur when a network attempts to store too many similar patterns (e.g., Derrick et al., 2000; Becker, 2005; Butz et al., 2006; Wiskott et al., 2006).

Within this series of models of pattern separation in the dentate gyrus, simplicity is generally the rule, and for good reason. That is, judicious choice of a few key cell types and pathways, simulating some fundamental properties of neuronal information processing, allows examination of how those properties may or may not be sufficient to generate interesting behaviors. As a result, most of the above-mentioned models have simplified their considerations of the dentate gyrus to include a single layer of principal cells—the granule cells—which receive inputs from entorhinal cortex (the perforant path), and produce output (the mossy fibers) projecting to CA3. As such, these models typically do not explore the role of the hilus in dentate gyrus function.

A few prior computational models have been developed that do incorporate various classes of hilar cells. These models typically include large numbers of simulated neurons with a high degree of anatomical and biophysical realism, including characteristics not only of granule cells, but also of other cell types, including hilar mossy cells and hilar interneurons. For example, Santhakumar et al. (2005) presented such a model, based on published quantitative data and descriptions in a model presented by Patton and McNaughton (1995), to test the idea that mossy fiber sprouting could lead to granule cell hyperexcitability. Similarly, Morgan et al.'s large-scale, biophysically realistic model considered how nonrandom connections between granule cells could produce hyperexcitable, seizure-prone circuits (Morgan et al., 2007; Morgan and Soltesz, 2008). However, these models did not specifically address pattern separation as an emergent function—although, of course, granule cell hyper-excitability would decrease sparsity of dentate gyrus outputs, thereby increasing overlap and decreasing pattern separation.

Lisman et al. have developed a series of computational models of the hippocampus, specifically considering how granule cell–mossy cell connections and CA3-mossy cell feedback connections could mediate sequence learning (Lisman, 1999; Lisman and Otmakhova, 2001). These models show how the convergence on granule cells of entorhinal afferents and of CA3 backprojections (via hilar mossy cells) could account for phase precession: the phenomenon in which, as a rat runs through a place field, the corresponding place cells fire with progressively earlier phase on each successive theta cycle (Lisman et al., 2005). Lörincz and Buzsáki (2000) have also suggested a role for the dentate gyrus hilus in sequence learning. Specifically, these authors suggested that excitatory granule cell–mossy cell–granule cell loops could form circuits with variable delays, allowing the dentate gyrus to perform temporal deconvolution, recovering temporal structure originally present in entorhinal inputs. Although these models of temporal and sequence learning do not specifically address pattern separation, these functions are not incompatible. Indeed, Lörincz and Buzsáki (2000) note that a subpopulation of mossy cells with "short" delays could operate primarily to help sparsify granule cell output, promoting pattern separation as well as temporal deconvolution.

However, as the above review suggests, there has to date been somewhat of a disconnect between the computational models of dentate gyrus function and pattern separation—most with fairly abstract models that focus primarily on granule cells—and computational models that include hilar cells but do not specifically address pattern separation. Here, we present a model of the dentate gyrus that begins to address this gap. This is a relatively small-scale, simplified model that builds on prior ideas of Marr, Rolls, and colleagues, but expands those

ideas to include not only granule cells, but also hilar cells, specifically the glutamatergic mossy cells and one of the major classes of hilar GABAergic neurons, the HIPP cells (i.e., *H*ilar *I*nterneurons with axons innervating the terminal zone of the *P*erforant *P*ath). Based on these considerations, it is suggested that hilar neurons such as the mossy cell and HIPP cell could influence granule cell activity in such a way that pattern separation could be better modulated in response to changing environmental demands—that is, so that pattern separation could be dynamically regulated.

DENTATE GYRUS ANATOMY AND PHYSIOLOCY

The dentate gyrus resembles other hippocampal and cortical networks in its basic elements, with a few notable exceptions. These differences may provide the dentate gyrus with a unique ability to perform pattern separation.

Like other cortical systems, the dentate gyrus includes a major class of principal cell, the dentate granule cell (labeled GC in Fig. 1), that uses glutamate as its primary neurotransmitter. Like the pyramidal cells of the hippocampus, the granule cells are packed within a discrete cell layer, called the granule cell layer (GCL, Amaral et al., 2007). The granule cell is highly polarized, with a large dendritic tree emerging from one pole, into the molecular layer. The major cortical afferent input to the dentate gyrus arises from Layer II of the entorhinal cortex. Layer II neurons from the lateral division of the entorhinal cortex terminate in the outer third of the molecular layer (OML), and Layer II cells in the medial entorhinal cortex innervate the middle third of the molecular layer (MML, Amaral and Witter, 1989). These axons “perforate” the subiculum on their path to the dentate gyrus, leading to the name “perforant path” (PP) for this projection. The inner third of the molecular layer (IML) is innervated by extrinsic afferents from the septum, mammillary bodies, and hilar cells (Seress, 2007); these hilar cells will be discussed further below.

Also in common with other cortical systems, the dentate gyrus contains various subtypes of GABAergic interneurons that innervate distinct parts of the granule cell body and dendritic tree; these include GABAergic neurons that primarily target the granule cell body (“basket” cells, BC), chandelier cells (CC) that innervate the axon hillock preferentially, and other types of interneurons. There are many other specific subtypes of interneuron, including those that innervate each other, synapse onto presynaptic terminals and regulate transmitter release, or are coupled by gap junctions. As in other cortical networks, the GABAergic neurons of the dentate gyrus still defy complete characterization, and there is some intersection between groups (Scharfman, 1992, 1995, 1999; Freund and Buzsáki, 1996; Houser, 2007). However, it can be argued based on structural and functional data that the most influential of these subtypes are (1) the interneurons responsible for “shunting” inhibition, the basket cells and chandelier cells, which target the soma or axon hillock of the granule cells, and (2) the interneurons that innervate the dendritic tree of granule cells, or inputs to the dendritic tree such as afferents from the entorhinal cortex.

Regarding the interneurons that innervate the granule cell dendritic tree, there are primarily two cell types: the GABAergic neurons that innervate the inner molecular layer (the so-called HICAP cells) and the HIPP cells that innervate the distal two-thirds of this layer. The former are relatively rare (Halasy and Somogyi, 1993; Freund and Buzsáki, 1996; Houser, 2007) and poorly understood, and so they are de-emphasized in the model. The HIPP cells have been studied much more, appear to be a substantial fraction of hilar neurons, and several experimental approaches suggest their importance, so they are emphasized here. However, it should be noted that there are some discrepancies concerning their characteristics, and there may be subtypes of HIPP cells. What is clear is that they have cell bodies located primarily within the hilus, with both dendrites and axons extending into the molecular layer (Halasy and

Somogyi, 1993). Although the major axonal projection is the molecular layer, primarily the distal two-thirds (Halasy and Somogyi, 1993), some of the axon collateralizes within the hilus (Deller and Leranth, 1990). Electron microscopy would suggest that their axons may innervate terminals of the perforant path, dendrites of granule cells (or other neurons), as well as other processes (Milner and Bacon, 1989; Deller and Leranth, 1990; Milner and Veznedaroglu, 1992). HIPP cells are notable for their expression of the peptides, neuropeptide Y, and somatostatin, but this characteristic has also led to some confusion, because some other GABAergic cell types express neuropeptide Y (Sperk et al., 2007), and expression changes under conditions of heightened activity (Sperk et al., 1992). Here, we use a conservative definition of HIPP cells that emphasizes their dominant attributes: (1) axonal projection to the molecular layer, primarily the distal two-thirds, and primarily granule cells, and (2) the potential to be activated by the perforant path as well as other cell types.

The granule cell axon ramifies extensively in the hilar region (for review, see Henze et al., 2002). The major branch of the granule cell axon descends into stratum lucidum of CA3, and courses parallel to the CA3 pyramidal cell layer, until it reaches CA2, where it ends. The part of the axon that courses through stratum lucidum gives rise to large, complex boutons periodically, and these “giant” boutons innervate the proximal dendrites of CA3 neurons as well as local interneurons. The giant boutons give the axon a “mossy” appearance, leading to the name “mossy fibers” or the “mossy fiber pathway” for the granule cell axon arbor. The giant boutons also exist in the hilus, where most terminate on the proximal dendrites of mossy cells. The mossy fibers have exceptional plasticity, exhibiting the capacity for axon outgrowth, long-term potentiation, and plasticity of peptide expression (including opiates, neuropeptide Y, neurotrophins, and even GABA; Jaffe and Gutiérrez, 2007).

These features of the mossy fibers make them unlike any other axon system in the hippocampus, and therefore they are likely to provide a key to the unique operations of the dentate gyrus. In fact, several prior computational models of the hippocampus have assumed that these giant mossy fiber synapses onto CA3 pyramidal cells could serve as “detonator” synapses, or “forcing inputs” (e.g., Marr, 1971; McNaughton and Morris, 1987; Rolls, 1989a,b, 2007; Treves et al., 2008). Empirically, it has been demonstrated that although a single presynaptic granule cell discharge may not suffice to cause postsynaptic CA3 pyramidal cell discharge, a train of spikes may suffice (Henze et al., 2002). Computationally, such forcing inputs would facilitate Hebbian learning between the pyramidal cell and any other coactive inputs, such as weaker excitatory inputs arriving along the direct entorhinal-CA3 pathway as well as collaterals from other CA3 pyramidal neurons. Thus, in these models, the mossy fiber synapses are a key component driving pattern storage in CA3.

In addition to innervating CA3 pyramidal cells, mossy fibers also make relatively dense excitatory synapses on GABAergic neurons, which in turn innervate CA3 pyramidal cells (Acsády et al., 2000). The GABAergic neurons that are innervated by mossy fibers include hilar interneurons, not just interneurons within CA3 (Acsády et al., 2000). This is important because the hilar interneurons are likely to discharge with low thresholds (Scharfman, 1991), potentially invoking feed-forward inhibition of CA3 neurons. The net effect is that CA3 pyramidal neurons are primarily inhibited under normal conditions (Acsády et al., 2000). However, the mossy fiber innervation of hilar interneurons is not a “detonator” synapse, and produces weak facilitation (Scharfman et al., 1990), in stark contrast to the large, facilitating input of the synapses involving the giant boutons onto mossy cells (Scharfman et al., 1990).

Besides the granule cells, the dentate gyrus has a unique second type of principal cell, the mossy cell (labeled MC in Fig. 1). Mossy cells, which have cell bodies in the hilus, receive their name because their cell bodies and proximal dendrites are covered with complex spines (thorny excrescences; Amaral, 1978). Mossy cells have large dendritic trees that span the hilus

(Scharfman and Schwartzkroin, 1988;Scharfman, 1999), and their axons project to many locations. There is local collateralization within the hilus, but the main projection is to the inner molecular layer. The major branch of the axon traverses the septotemporal extent of the hippocampus ipsilaterally and terminates in the inner molecular layer. It also projects to the homotopic dentate gyrus contralaterally. The longitudinal projection is often referred to as the associational projection, and primarily innervates granule cells (Buckmaster et al., 1996). Mossy cells also innervate GABAergic interneurons (Scharfman, 1995). The effects of mossy cells on granule cells may be conditional, because depolarization appears most robust when granule cells are depolarized concurrently, as might occur when a concomitant noradrenergic stimulus reaches the dentate gyrus (Scharfman, 1995;Harley, 2007).

An important aspect of the mossy cell–granule cell circuit is the potential for "runaway" excitation, or an escalation of excitatory activity due to positive feedback between granule cells and mossy cells. Presumably, this is ordinarily controlled by concomitant activation of inhibitory neurons by both granule cells and mossy cells. However, mossy cells appear less inhibited than granule cells normally, and are more depolarized normally (Otis et al., 1991; Scharfman, 1992). For these and other reasons that continue to be debated (Freund et al., 1992; Leranth et al., 1992), the mossy cells are vulnerable to excitotoxicity (Scharfman, 1999).

Given that other hippocampal cell fields, and indeed other cortical circuits, do not contain a cell type analogous to a mossy cell, and given the potential for positive feedback in the dentate gyrus due to the mossy cell–granule cell connectivity (Buckmaster and Schwartzkroin, 1994; Jackson and Scharfman, 1996), it seems reasonable to suggest that the mossy cells must impart a specialized function to the dentate gyrus that no other hippocampal subfield requires. The current model investigates whether mossy cells—and particularly the mossy–granule circuit —may provide distinct functionality, such as improved pattern separation.

THE DENTATE GYRUS MODEL

The basic goal of the model is to provide a framework to investigate how granule cells and hilar cells might interact to contribute to pattern separation. The model focuses on four basic cell types: granule cells, mossy cells, HIPP cells, and the other inhibitory interneurons (such as basket cells and chandelier cells). For simplicity, the model uses "point neurons" with no internal geometry, which are updated synchronously, and has four key parameters (discussed below) governing the behavior and influence of each cell type. It is important to emphasize the advantage of using such a simple model with a very limited number of free parameters is that it allows systematic exploration of how each of these parameters affects behavior. Although such a simple model will obviously not capture all the exquisite anatomical and physiological complexity of the dentate gyrus, it does allow testing of the hypothesis that a few key elements of the dentate network are sufficient to capture some aspects of the empirical data. If correct, the model would suggest overarching principles that can guide further research, and suggest a foundation upon which additional complexity can be added.y

Fundamental Elements of the Model

A schematic of the model is provided in Figure 1B; full details of the implementation are given in the Appendix. The model contains 500 simulated granule cells, a scale that represents ~1/2,000 of the ~1 million granule cells in rats (West et al., 1991; Rapp and Gallagher, 1996); the number of granule cells may be 2–4 times greater in humans (Seress, 2007). This number provides adequate power to explore pattern separation while maintaining computational tractability. In the model, the granule cell population is divided into nonoverlapping clusters, roughly corresponding to the lamellar organization along the

septotemporal extent of the dentate gyrus. The 500 cells in the model have been divided into 25 clusters, with each cluster containing 20 granule cells.

The model also contains inhibitory interneurons, labeled INT in Figure 1B, that represent the inhibitory influence of various GABAergic interneurons, such as the basket cells and chandelier cells. There is one interneuron per granule cell cluster in the model. Each interneuron is activated by granule cells in the cluster and in turn projects back to inhibit granule cells in that cluster, implementing a form of "winner-take-all" competition in which all, but the most strongly activated granule cells in a cluster are silenced. Given 25 clusters in the model, with approximately one granule cell winning the competition in each cluster, this means that ~25 of 500 (5%) of granule cells remain active in the model; this is consistent with estimates of 2–5% granule cell activity in the substrate (see Treves et al., 2008, for review).

The model also includes simulated hilar mossy cells and HIPP cells. Estimated cell counts for these hilar cell types vary, with 30,000–50,000 hilar mossy cells in rats (West et al., 1991; Buckmaster and Jongen-Relo, 1999), leading to a ratio of about 3–5 mossy cells per 100 granule cells. Therefore, the model includes 20 mossy cells per 500 granule cells. Cell counts for hilar interneurons are especially variable, but a recent estimate (Buckmaster and Jongen-Relo, 1999) suggests about 12,000 HIPP cells, or less than 2 HIPP cells per 100 granule cells. To reflect these empirical data, the model includes 10 HIPP cells.

External input to the model comes from 100 afferents representing entorhinal input (the perforant path); this 1:5 ratio of entorhinal afferents to granule cells is consistent with estimates of the cells of origin of the perforant path, reaching ~200,000 Layer II entorhinal neurons in rat (Amaral et al., 1990). Perforant path-granule connectivity is sparse in the substrate, with each granule cell receiving input from about 2% of entorhinal Layer II neurons, with an estimated 400 entorhinal inputs (10% of the total) required to discharge one granule cell (McNaughton et al., 1991). Since the model assumes only 100 entorhinal inputs, strict adherence to this ratio would mean that each granule cell would only receive input from about two entorhinal neurons, which in turn would make it impossible for the granule cell to become active if fewer than 50% of its entorhinal afferents were active. This is an example of scaling difficulties inherent in computational models, where the number of simulated neurons and connections are only a fraction of those existing in the substrate. As a compromise, the model assumes that each granule cell in the model receives input from a random 20% of the entorhinal afferents from Layer II; each granule cell can become active in response to activation of about 10% of the afferents to that granule cell.

Another difficult question is what level of perforant path activation is "normal"—that is, what percentage of perforant path afferents are active in vivo in response to a given stimulus input. Some studies have suggested that dentate granule cells require input from an estimated 10% of the 4,000 perforant path afferents that contact a given granule cell in rat (McNaughton et al., 1991), which in turn suggests that 10% of Layer II entorhinal neurons are normally activated above threshold. This number may be high because it was based on experimental data that involve applied stimulation, not physiological stimulation. The simulations reported here assume that the percentage of perforant path afferents which are active to represent a given stimulus input (called the input density, *d*) is normally about 10%, but can range from 1 to 20%, depending on the specific task being simulated.

The sequence of events in the model is as follows: on each trial, a pattern of perforant path inputs, representing entorhinal Layer II neuron discharge, can evoke suprathreshold activation (an action potential) in granule cells; inhibitory interneurons are then activated and silence all but the most strongly activated granule cell(s) within a cluster.

Granule cells also excite mossy cells in the model, and the mossy cells in turn provide distributed feedback excitation to granule cells. The perforant path input also directly activates HIPP cells that provide inhibition to the granule cells. Any granule cell *j* that remains active after all net excitatory and inhibitory conductances have been integrated produces output $y_j > 0$ (suprathreshold activation); for all other granule cells $y_j = 0$ (subthreshold activation). This final pattern of granule cell outputs is the external output of the model to the given input pattern. Pattern separation is achieved if the average overlap among the output patterns is less than the average overlap among the input patterns.

The model uses simple "point neurons," with membrane potential computed as a balance between opposing forces of inhibition and excitation. The current model does not incorporate many additional complexities of granule, mossy and HIPP cells, such as projections from mossy cells to interneurons, mossy cell dendrites extending into the GCL, the effects of subthreshold activity, peptides, etc. One reason to refrain from adding these elements here is that they seem least critical, based on the existing evidence. For example, despite the fact that the molecular layer dendrite of mossy cells seems important (Scharfman, 1991), it is not a characteristic of all mossy cells. Although mossy cell innervation of interneurons is clear, this projection is not well understood. Although subthreshold activity is undoubtedly important, it can be argued that this is in part embodied in the constants employed in the model, and in addition, the ultimate output of a circuit involves suprathreshold discharge. Although these and other features of the substrate are undoubtedly important, our focus here is on the interaction between hilar mossy and HIPP cells and the granule cells, and the degree to which this interaction could produce pattern separation in the dentate gyrus.

Implementation of the Model

Given the quantitative information used as a basis for the model, and other assumptions described above, the model's ability to perform pattern separation on a defined group of inputs is affected by four key free parameters, one associated with each cell type, which can be manipulated to simulate physiological manipulations. Table 1 summarizes these key parameters along with the "default" values used in the simulations presented here. (The default values were chosen to maximize pattern separation in the model; the effects of parametric manipulation are discussed further below, and in the Appendix.) In brief, V_{rest} is a constant that defines the resting potential of granule cells in the absence of any perforant path input; it is inversely related to the "threshold" that granule cells must reach in order to fire. β_{INT} is a constant representing the strength with which local interneurons inhibit granule cells. β_{HIPP} and β_{MC} are constants that represent the global influence on granule cells of HIPP cells and mossy cells, respectively. Equations incorporating these constants are given in the Appendix, but conceptually these constants can be interpreted as the relative strength by which various excitatory and inhibitory processes affect activity in granule cells. As such, changing these constants (as could be the case if there is a modulation of the network by inputs that selectively target a particular cell type, such as mossy cells or interneurons) simulates a global increase or decrease in the influence of these cell types in the network. It is important to note that these parameters are in arbitrary units; in other words, an increase of V_{rest} from 20.30 to 20.15 in the model does not necessarily correspond to an increase of 0.15 mV or any other physical unit. Rather, by increasing and decreasing each of these parameters in the model, it is possible to explore how increasing and decreasing corresponding influences in the biological substrate could affect network performance and therefore affect pattern separation in the dentate gyrus.

An important aspect of dentate gyrus function is long-term plasticity, by which connections—particularly from perforant path afferents to granule cells—are modified. Others have noted that such plasticity may facilitate the network's ability to perform pattern completion, for example, by implementing a competitive network (e.g., Rolls, 2007). Existing models of the

dentate gyrus often assume Hebbian learning rules, facilitating function as a competitive network in which the sum of synaptic weights on each neuron remain relatively constant during learning (e.g., Levy, 1985; Levy and Desmond, 1985; Rolls, 1989a,b, 2007). A similar Hebbian learning rule that incorporates features of long-term potentiation and depression could be incorporated into the current model. However, such a function is most likely to be relevant in situations in which stimuli are presented repetitively, for example, across iterative conditioning trials; by contrast, the current model is not applied to learning per se, but rather to patterns presented in single instances. Accordingly, plasticity is not considered in the current model.

Pattern Separation in the Model

Before proceeding, in the next section, to compare the results of the model against empirical data, it is important to clarify how the model performs pattern separation. Figures 2A–D show a simple example of pattern separation using the model. Figure 2A illustrates a sample pattern of activity along the 100 perforant path afferents. In Pattern 1, 7 of the 100 afferents are active (to facilitate illustration, these have been grouped to the left of the figure). Figure 2B shows a second input pattern that overlaps substantially with the first input pattern: Pattern 2 also has seven active afferents, six of which are the same as in Pattern 1. The remaining 92 afferents are silent in both patterns. Thus, percent overlap between the two patterns is [(6 + 92)/100] 3 100 = 98%. (In information processing terms, percent overlap equals (N-HD) × 100, where HD is the Hamming distance between the patterns, defined as the absolute differences in response to each pattern, summed across all N elements in the pattern.)

Figure 2C illustrates the network output, in terms of granule cell activity along the mossy fibers, in response to Pattern 1 (for simplicity, only the first 100 of the 500 granule cells are shown in the figure; the remaining 400 show similar characteristics). Figure 2D illustrates the network output to Pattern 2.In each case, a similar percentage of granule cells are active in response to each pattern, but the identity of these cells differs from pattern to pattern. Across all 500 granule cells, overlap in response to the two patterns is 68.39%. This is about a 30% reduction in overlap in the output to the two patterns, compared to the 98% overlap that was present at the inputs. Thus, the dentate gyrus network has performed pattern separation by reducing overlap.

The examples shown in Figures 2A,B are extreme, in that they show two patterns with very high overlap. A less extreme example would be patterns in which, say, a random percentage or density *d* of perforant path afferents are active. Figure 2E shows the average percent overlap, at input and at output (after processing by the dentate gyrus model), for various sets of 10 patterns. For a set of input patterns in which 10% of the elements are active (d = 10%), average percent overlap is a little more than 80%; after processing by the dentate gyrus network, average percent overlap falls to about 65%. This reduction in overlap is the result of pattern separation by the dentate gyrus model.

Figure 2E also shows similar calculations for sets of 10 input patterns, constructed with different input densities. For input patterns with very sparse firing density (e.g., d = 1 or 5%), there is very high percent overlap at the inputs, because most afferents are silent during all input patterns; under these conditions, dentate gyrus processing does reduce overlap somewhat, but not too much. For patterns with very high firing density (e.g., d = 20% or more afferents active), percent overlap measured at the outputs is actually higher than the overlap present at the inputs. Note that this does not mean that the output patterns cannot be distinguished; it merely means that there is no relative benefit to dentate gyrus processing in this case.

One immediate prediction of the model, evident from Figure 2E, is therefore that the benefits of dentate gyrus processing should be greatest for a low-to-moderate proportion of active entorhinal inputs. As the number of active perforant path afferents grows past some maximum

(perhaps by overstimulation of the perforant path or by inhibition of entorhinal cortex Layer II interneurons), this benefit may be lost.

COMPARISON OF THE MODEL TO EXPIRICAL DATA

Originally, the proposal that the dentate gyrus network could perform pattern separation was based on computational arguments, leading to the prediction that tasks that require disambiguation of highly overlapping inputs should be particularly dependent on dentate gyrus function, and should be impaired following dentate gyrus lesions.

Only recently has empirical evidence emerged to support this idea. For example, Gilbert et al. (2001) considered a spatial delayed match-to-sample task in which rats were challenged to choose a previously baited food well in preference to another food well at a different location; the two locations could be distant or closely spaced. Gilbert et al. argued that rats solve this task based on distal environmental cues, and that this information begins to overlap—or become more difficult to distinguish—if the wells are closely spaced. Under these conditions, pattern separation by the dentate gyrus should be critical. And, as predicted, rats with dentate gyrus lesions indeed showed impaired performance at this task—and their impairment grew progressively greater as the spatial separation between the two wells decreased. These behavioral data are consistent with the idea that the dentate gyrus plays a key role in pattern separation, especially of sensory inputs that are of overlapping or ambiguous. Similarly, a recent human functional neuroimaging study showed that an area including the dentate gyrus and CA3 was the only medial temporal area that appeared to distinguish between previously viewed photos and slight variations of those images (Bakker et al., 2008). The authors argued that these data support the idea of a pattern separation function in dentate gyrus, in which small differences in inputs are translated into large differences in the outputs.

In addition to behavioral data from lesioned animals, and functional imaging data from humans, electrophysiological data are also emerging that are consistent with the idea of pattern separation in the dentate gyrus. The next section reviews one such study, and shows how the model can address these data.

Testing the Model

Leutgeb et al. (2007) tested the ability of dentate gyrus granule cells to disambiguate small differences in cortical input patterns, by recording from hippocampal CA3 and dentate place cells as rats explored a series of environments (numbered 1–7) that included a square enclosure (Environment 1), a circular enclosure (Environment 7), and several intervening enclosures (Environments 2–6) that gradually “morphed” between these two extremes. CA3 place cells that were active in the square environment (Environment 1) showed hysteresis: a relatively smooth transition as the environment changed from square, through the intervening stages (Environments 2–6), to circular (Environment 7). By contrast, dentate gyrus place cells (presumed granule cells) showed strong decorrelation between even the most similar of the morphed environments; in fact, the correlation of place cell firing for two neighboring environments (e.g., 1 vs. 2) was no greater than for the two extremes (1 vs. 7). Thus, extremely similar inputs were transformed into distinct patterns of granule cell activation. This pattern separation appeared to originate in the dentate gyrus, because perforant path inputs from the entorhinal cortex had grid-like firing fields that did not exhibit detectable changes as the environment was incrementally transformed (Leutgeb et al., 2007). More recently, Hunsaker et al. (2008) showed that selective dentate lesion (including some hilar damage) disrupted the ability to detect a change of environment from circle to square as well as the ability to detect changes in local cues within an environment; lesions of CA3a,b disrupted the latter but not the former, consistent with the premise that dentate gyrus is particularly critical for detecting small changes.

The "morphed environments" of Leutgeb et al. (2007) can be approximated in the model by considering a set of overlapping input patterns, and evaluating the responses of individual dentate granule cells to each. Specifically, two patterns (1 and 7) were constructed so that each had seven active entorhinal inputs, only one of which was active in both patterns. Five intervening patterns were then constructed to gradually "morph" between Patterns 1 and 7, as shown in Figure 3A. Therefore, pairs of "neighboring" patterns, such as Pattern 1 and Pattern 2, or Pattern 2 and Pattern 3, overlapped extensively, each pair having an average overlap of 98%. But Patterns 1 and 7 had overlap of only 88% (Fig. 3B, "Input"). Overall, the input patterns had average overlap of 94.7%.

Patterns 1–7 were presented to the dentate gyrus model in sequence, and the model's output to each was recorded. Overall, the output patterns averaged 85% overlap, less than the 94.7% average overlap of the inputs; this reduction in percent overlap indicates that the dentate gyrus network performed pattern separation on this set of highly overlapping inputs. However, pattern separation did not occur equally for all pairs of inputs. Instead, the dentate model tended to produce most separation on pairs of patterns that had originally overlapped the most. Figure 3B shows the percent overlap, computed across the granule cell outputs, for different pairs of patterns. Patterns 1 and 2, which were highly overlapping, were made quite a bit less similar. But Patterns 1 and 7, which were already fairly distinct, were not made more distinct by dentate processing. In other words, the dentate gyrus model produces the most pattern separation for inputs that are highly similar; there is relatively less benefit from dentate gyrus processing for inputs that are already quite distinct. This could produce the behavioral effects shown by Gilbert et al. (2001), where animals with dentate lesions were particularly impaired in distinguishing inputs with low spatial separation, but were about as good as controls on distinguishing inputs with high spatial separation, and presumably quite distinguishable.

One way of assessing the ability of the dentate gyrus to selectively perform pattern separation on highly overlapping inputs is to look at how closely correlated neuronal responses are to two patterns; if the responses of individual granule cells are very similar to the two patterns, then little pattern separation is likely to have occurred. In the rats, Leutgeb et al. (2007) demonstrated that, as the animals were placed in the progressively changing ("morphed") environments, CA3 activity was highly correlated in neighboring Environments 1 and 2; this correlation decreased approximately linearly as the difference between environments increased, reaching a minimum for the least-similar Environments 1 and 7. By contrast, there was less correlation in dentate responses for environments that were extremely similar (Fig. 4A). This lack of correlation in the responses of individual granule cells to highly overlapping inputs means that pattern separation is occurring as the dentate gyrus transforms highly overlapping input patterns into less-overlapping output patterns. On the other hand, Figure 4A shows that, for the most distinct environments, the correlation in the dentate gyrus was about the same as in CA3—indicating once again that dentate gyrus processing appears specialized to perform the greatest degree of pattern separation on the mostly highly overlapping input patterns.

A similar effect arises in the model, presented with the seven input patterns shown in Figure 3A. The "Input" line in Figure 4B represents the correlation between entorhinal afferents in the seven input patterns, and thus represents a kind of "baseline" correlation. For highly similar input patterns (e.g., Patterns 1 and 2), input correlation is high; correlation decreases linearly as patterns become more dissimilar, reaching a minimum for the most-dissimilar Patterns 1 and 7. The "Output" line in Figure 4B shows the correlation in dentate granule cell outputs, for each pair of patterns. For highly similar input Patterns 1 and 2, the correlation in granule cell outputs is less than the correlation in the inputs, indicating that pattern separation has occurred. Although correlation decreases as the input patterns become more distinct, it does not decrease linearly, so that for the most distinct inputs (Patterns 1 and 7), the correlation in dentate granule cell responding is no lower than the correlation of the original entorhinal

afferents. In other words, in the model as in the rats, dentate gyrus processing selectively reduces correlation in responding to highly overlapping inputs, but has less effect on correlation in responding to inputs that were already highly distinct.

What underlies this pattern separation phenomenon in the rat and in the model? One factor may be the ability of the individual dentate granule cell to respond in markedly different ways to extremely similar inputs. Leutgeb et al. (2007) reported that rat dentate gyrus place cells can have multiple place fields within a single environment, and that place field responses can be markedly different in similar environments. This is in contrast to the hysteresis exhibited by CA3 place fields. Figure 5A shows the responses of some individual dentate granule cells to analogous locations in the seven morphed environments. Some cells show relatively smooth linear change as the animal moves from one environment to the next, but other cells show nonlinear and even biphasic response curves. Figure 5B illustrates analogous response curves from granule cells in the model, using input Patterns 1–7. Some cells (left) respond similarly to neighboring patterns. But others show nonlinear response curves, responding very differently to one pattern than to its neighbors, or biphasic response curves, responding strongly to several nonadjacent patterns. This lack of hysteresis in the granule cells in the model parallels the same phenomenon observed in vivo, and underlies the ability of the model to provide different outputs to similar inputs.

In the model, this lack of hysteresis is accomplished partly by feedback from the hilus to the granule cells. In the model, both hilar mossy cells and HIPP cells project sparsely, and in a distributed fashion, to the granule cells. This means that one pattern of activity across the perforant path afferents can excite HIPP cells that project to very different subgroups of granule cells; small differences in the input can therefore be magnified by HIPP cells to produce inhibition in widely distributed populations of granule cells. Similarly, a mossy cell that is excited by one granule cell will feed back to excite a widely distributed network of granule cells, which again means that inputs that initially evoke activity in overlapping granule cell populations may be redistributed to activate substantially different granule cell populations.

As such, a prediction of the model is that lesioning or disrupting the hilus should profoundly affect pattern separation, particularly for highly similar inputs.

Effects of Hilar Lesion or Dysfunction

There are very few studies that address the specific effects of hilar lesions on the dentate gyrus network, and, more specifically, on pattern separation. In the 1980s, a paradigm was developed to selectively lesion hilar cells by electrical stimulation of the dentate gyrus in vivo, using anesthetized rats (reviewed in Sloviter et al., 2003). Stimulation that evoked large amplitude population spikes in granule cells led to neuronal loss almost exclusively in the hilar region, with many of the GABAergic interneuron subtypes surviving. Following the procedure, perforant path-evoked population spikes in the GCL demonstrated a loss of paired pulse inhibition (Sloviter et al., 2003). The results suggested that mossy cells were critical to maintain granule cell inhibition. Subsequently, a modification to this protocol was used in hippocampal slices, and it was noted that loss of hilar neurons led to burst discharges in area CA3 (Scharfman and Schwartzkroin, 1990a,b). Taken together, the studies suggested that hilar neurons could profoundly influence the granule cell responses to perforant path stimulation, and hilar damage would produce increased excitability in the granule cell population as well as increased synchrony in the CA3 population.

Subsequent studies began to dissociate the effects of hilar mossy cells from GABAergic interneurons. For example, Ratzliff et al. (2004) performed a specific ablation of a subset of hilar mossy cells or interneurons in hippocampal slices. The results, shown in Figure 6A, suggested that mossy cell ablations caused a decrease in the field potential representing granule

cell activation in response to perforant path stimulation; in contrast, lesions to a subset of hilar interneurons caused an increase. These data are consistent with studies suggesting that mossy cells primarily innervate granule cells and are excitatory (Soriano and Frotscher, 1994; Scharfman, 1995).

Similar lesions can be simulated in the model by selectively disabling the mossy cells or HIPP cells, and then testing the model with a series of patterns to observe granule cell activity. To accomplish this, the model was presented with a set of 10 input patterns, each randomly constructed to have 10% input firing density (i.e., a random 10 of 100 elements active in each pattern). Figure 6B shows that, in the model as in the slice, mossy cell ablation reduces granule cell activity, relative to control (preablation) levels; HIPP cell ablation increases granule cell activity. The increase in granule cell activity in the model following HIPP cell ablation is less than that observed in the slice, presumably because the HIPP cells are not the only cells that innervate granule cells, and some of the hilar interneurons lesioned in the slice were non-HIPP cells.

Similarly, the reduction in granule cell firing in the model following loss of mossy cell function is greater than the reduction observed in the slice. Some of this difference may be due to the fact that mossy cell innervation of interneurons is not considered in the model. It is also the case that the output in the model is suprathreshold, but the output in the study of Ratzliff et al. is a combination of subthreshold and suprathreshold activity. Another explanation is based on the fact that only a subset of mossy cells was lesioned in the slice. Ratzliff et al. (2004) estimated that their technique might have ablated 5–22% of the mossy cells in a 350-μm slice. On the other hand, because mossy cell axons ramify so widely, the slice preparation itself possibly represents a dramatic decrease in “normal” levels of mossy cell influence on granule cell activity.

To determine if the differences between the model and the empirical data are simply due to the number of mossy cells involved, it is possible to selectively reduce a fixed percentage of mossy cells in the model, and determine if the effect on granule cell activity is closer to the results of the study by Ratzliff et al. Figure 6C shows that the average granule cell discharge in the model declines with depletion in mossy cell number; as would be expected, there is a gradual decrease in granule cell activity as mossy cell count drops.

Another way to manipulate hilar function in the model is by leaving the hilar cells intact, but reducing their global effect on granule cells. This can be done by altering the free parameters, β_{MC} and β_{HIPP} which define how strongly mossy cells and HIPP cells affect granule cells. Physiologically, this could occur by many different mechanisms, including downregulating hilar cell activity and/or downregulating the effectiveness of hilar neuron synapses onto granule cells. Figure 7A shows that, in general, reducing β_{MC} from its “default” value leads to a reduction in granule cell activity, similar to the effects of physically lesioning mossy cells in the model (compare Fig. 6C). Downregulating HIPP cell effects on granule cells by reducing β_{HIPP} generally increases granule cell activity, analogous to the effect of physically lesioning HIPP cells in the model (compare Fig. 6B). Figure 7A also shows that there is an intermediate operating range, near the “default” values for each parameter, when these two opposing excitatory and inhibitory effects are balanced. Figure 7B shows the effect of these same manipulations on pattern separation: average percent overlap, measured at the outputs for a series of 10 random patterns (constructed with input density $d = 10\%$) tends to be lowest when both mossy cell and HIPP cell function are near their default values.

The conclusion to be drawn from Figure 7B is that hilar cell upregulation and downregulation can be an effective way to modulate pattern separation in the model. Pattern separation can be strongly decreased by decreasing mossy cell function and/or by increasing HIPP cell function;

pattern separation can be mildly increased by the opposite manipulations. This raises the possibility that similar manipulations of hilar function in the substrate could dynamically regulate pattern separation in the behaving animal as it explores and interacts with its environment.

DISCUSSION

The model presented here provides a framework to systematically explore a role for hilar cells in pattern separation. Specifically, the model incorporates two of the most common and potentially powerful cell types in the hilar region: the excitatory hilar mossy cells and the GABAergic HIPP cells. The model is a relatively simple one, reducing the complexity of cell types, connectivity, and physiology, based on evidence from the literature that suggests the most important network characteristics. In addition, the model simplifies complexities of circuitry associated with the differences across septotemporal axis. By focusing on a few key classes of neurons, and simplified functions of each, the model suggests that hilar mossy and HIPP cells may be sufficient for dynamic regulation of pattern separation in the dentate gyrus. This, of course, does not prove that they are necessary, or rule out additional ways in which pattern separation may be regulated in the dentate gyrus.

The model provides an interpretation of several recent empirical findings, including the idea that the dentate gyrus is most critical when the organism must discriminate between highly overlapping inputs, but less critical when the inputs are readily distinguished (Gilbert et al., 2001), and the finding that population correlations in dentate granule cells are reduced more for extremely similar inputs than for inputs that differ greatly (Leutgeb et al., 2007). These simulation results, while important, might be replicated by a number of other, previous models that have considered how the GCL might produce pattern separation; however, prior models typically focused on granule cells without specifically considering a role for hilar cells in this process.

The novel contribution of the current model is to lay the foundation for the premise that hilar cells play a significant role in this pattern separation process. By including hilar mossy cells and HIPP cells, which provide excitation and inhibition respectively to granule cells in the model in discrete ways, the model is capable of accounting for data showing that selective ablation of hilar mossy cells has the effect of reducing population spike amplitude among dentate granule cells, while ablation of hilar interneurons increases it (Ratzliff et al., 2004)—and the model further predicts that by modulating the effect of these hilar cells, the degree of pattern separation can be dynamically upregulated or downregulated. Specifically, as shown in Figure 7, pattern separation (defined as a decrease in overlap in patterns processed by the dentate gyrus model) is generally increased when mossy cell influence is strong, and HIPP cell influence is weak.

This possibility begs a very important question: would it ever be desirable not to perform maximal pattern separation? One example of a condition when pattern separation might be best minimized would be a task in which effective behavior requires ignoring (rather than emphasizing) small variations in input stimuli. An example of such a task would be category learning, in which multiple different stimuli are to be treated similarly based on their commonalities, rather than their differences. In such a case, downregulation of pattern separation might improve performance.

A study that provides possible support for this hypothesis showed that mice with a deletion in the gene for the serotonin-5-HT1A receptor have decreased ability to discriminate ambiguous tones (Tsetsenis et al., 2007). The same study showed that the phenotype could be reversed by application of serotonin in a line of mice expressing 5-HT1A receptors only in the dentate gyrus. This study suggests a role of postnatal neurogenesis, ecause 5-HT1A receptors mediate

the well-known facilitation of neurogenesis by serotonin (Brezun and Daszuta, 1999; Radley and Jacobs, 2002; Encinas et al., 2006). It is consistent with the idea that postnatal neurogenesis allows the dentategyrus to respond to fine differences in inputs, enhancing functions like pattern separation, by providing new populations of granule cells throughout adulthood (Treves et al., 2008). More relevant here is that this study suggests the possibility that neuromodulators such as serotonin may provide a mechanism to upregulate and downregulate pattern separation in the dentate gyrus, by short-term effects on target neurons, by longer-term effects on adult neurogenesis, or both. This process could be mediated, at least in part, by the hilus, as suggested by the fact that newly born neurons in the dentate gyrus, like their older counterparts, make projections directly to hilar neurons, and receive inputs from them (Zhao et al., 2008).

There are other potential candidates that could also contribute to dynamic regulation of pattern separation in the dentate gyrus. For example, there are strong projections to dentate gyrus from the medial septal/diagonal band (MS/DB) complex; these include both GABAergic and cholinergic fibers, which have been suggested to modulate granule cell activity (e.g., Deller et al., 1999; Leranth and Hajszan, 2007). Importantly, many of these projections target mossy cells and GABAergic neurons of the dentate gyrus, including HIPP cells (Deller et al., 1999; Dougherty and Milner, 1999; Gulyás et al., 1999). In prior modeling work, we have suggested that the hippocampus may operate in a self-regulating feedback loop with the MS/DB, with high novelty and/or prediction error in the hippocampus resulting in higher influx of acetylcholine (ACh) from the MS/DB, which in turn could facilitate LTP in hippocampus (Myers et al., 1996, 1998; Rokers et al., 2000). Such an increased influx of ACh from the MS/DB to dentate gyrus—potentially via hilar neurons—might also encourage pattern separation and/or plasticity, which in turn might help the hippocampus to store new information under conditions of high novelty or unpredictability.

Hippocampal field CA3 also sends “backprojections” to the hilus (for review, see Scharfman, 2007b), and these backprojections could provide yet another mechanism for the hippocampus to self-regulate its inputs from dentate gyrus. This should be explored in future modeling efforts, with the expectation that area CA3 backprojections would allow pattern separation to be maximized under conditions where the organism is required to differentiate highly similar inputs, perhaps by learning different behavioral responses to similar sensory stimuli, and allow pattern separation to be minimized in conditions where various stimuli are to be mapped to similar behavioral responses, facilitating generalization among those stimuli. Consistent with this idea, Hunsaker et al. (2008) found that selective lesions of CA3c, a major source of backprojections to dentate gyrus, were sufficient to disrupt the ability to detect small, local changes within an environment, but did not disrupt the ability to detect large changes in the overall shape of an environment.

Such ideas of dynamic regulation of pattern separation can also be tested using empirical techniques in which the behaving animal is required to distinguish, or generalize among, various stimuli while challenged with manipulations (such as serotonin depletion or loss of CA3 backprojections) that alter hilar function. Based on the results of such studies, the current model could also be expanded as needed, by adding additional elements such as additional cell types (such as specific classes of inhibitory cell), additional connectivity to existing cell types (such as perforant path inputs to mossy and HIPP cells), and more detailed physiological characteristics (such as considering specific synapses with 5-HT1A or other receptor types). The model could also be extended to include a network representing hippocampal CA3, and allowing the two systems to interact. At present, though, the simplicity of the current model suggests that greater understanding of dentate gyrus function can be achieved by a relatively abstract exploration of hilar function, and that this hilar function is an important aspect of dentate gyrus that should receive more attention both in the context of computational modeling and empirical studies.

REFERENCES

Acsády L, Káli S. Models, structure, function: The transformation of cortical signals in the dentate gyrus. Prog Brain Res 2007;163:577–599. [PubMed: 17765739]

Acsády L, Katona I, Marítnez-Guijarro FJ, Buzsáki G, Freund TF. Unusual target selectivity of perisomatic inhibitory cells in the hilar region of the rat hippocampus. J Neurosci 2000;20:6907–6919. [PubMed: 10995835]

Amaral D. A Golgi study of cell types in the hilar region of the hippocampus in the rat. J Comp Neurol 1978;182(4 Part 2):851–914. [PubMed: 730852]

Amaral DG, Witter MP. The three-dimensional organization of the hippocampal formation: A review of anatomical data. Neuroscience 1989;31:571–591. [PubMed: 2687721]

Amaral DG, Ishizuka N, Claiborne B. Neurons, numbers and the hippocampal network. Prog Brain Res 1990;83:1–11. [PubMed: 2203093]

Amaral DG, Scharfman HE, Lavenex P. The dentate gyrus: Fundamental neuroanatomical organization ("Dentate gyrus for dummies"). Prog Brain Res 2007;163:3–22. [PubMed: 17765709]

Andersen, P.; Morris, R.; Amaral, D.; Bliss, J.; O'Keefe, J., editors. The Hippocampus Book. Oxford, UK: Oxford University Press; 2006.

Bakker A, Kirwan CB, Miller M, Stark CE. Pattern separation in the human hippocampus and dentate gyrus. Science 2008;319:1640–1642. [PubMed: 18356518]

Becker S. A computational principle for hippocampal learning and neurogenesis. Hippocampus 2005;15:722–738. [PubMed: 15986407]

Brezun JM, Daszuta A. Depletion in serotonin decreases neurogenesis in the dentate gyrus and the subventricular zone of adult rats. Neuroscience 1999;89:999–1002. [PubMed: 10362289]

Buckmaster PS, Jongen-Relo AL. Highly specific neuron loss preserves lateral inhibitory circuits in the dentate gyrus of kainite-induced epileptic rats. J Neurosci 1999;19:9519–9529. [PubMed: 10531454]

Buckmaster PS, Schwartzkroin PA. Hippocampal mossy cell function: A speculative view. Hippocampus 1994;4:393–402. [PubMed: 7874231]

Buckmaster PS, Wenzel HJ, Kunkel DD, Schwartzkroin PA. Axon arbors and synaptic connections of hippocampal mossy cells in the rat in vivo. J Comp Neurol 1996;366:271–292. [PubMed: 8698887]

Butz M, Lehmann K, Dammasch IE, Teuchert-Noodt G. A theoretical network model to analyse neurogenesis and synaptogenesis in the dentate gyrus. Neural Netw 2006;19:1490–1505. [PubMed: 17014989]

Chawla MK, Barnes CA. Hippocampal granule cells in normal aging: Insights from electrophysiological and functional imaging experiments. Prog Brain Res 2007;163:661–678. [PubMed: 17765744]

Cohen, N.; Eichenbaum, H. Memory, Amnesia and the Hippocampal System. Cambridge, MA: MIT Press; 1993.

Deller T, Leranth C. Synaptic connections of neuropeptide Y (NPY) immunoreactive neurons in the hilar area of the rat hippocampus. J Comp Neurol 1990;300:433–437. [PubMed: 2266195]

Deller T, Katona I, Cozzari C, Frotscher M, Freund T. Cholinergic modulation of mossy cells in the rat fascia dentata. Hippocampus 1999;9:314–320. [PubMed: 10401645]

Derrick BE. Plastic processes in the dentate gyrus: A computational perspective. Prog Brain Res 2007;163:417–451. [PubMed: 17765732]

Derrick BE, York AD, Martinez JL. Increased granule cell neurogenesis in the adult dentate gyrus following mossy fiber stimulation sufficient to induce long-term potentiation. Brain Res 2000;857:300–307. [PubMed: 10700582]

Dougherty KD, Milner TA. Cholinergic sepatal afferent terminals preferentially contact neuropeptide Y-containing interneurons compared to parvalbumin-containing interneurons in the rat dentate gyrus. J Neurosci 1999;19:10140–10152. [PubMed: 10559422]

Eichenbaum, H. The Cognitive Neuroscience of Memory. New York: Oxford University Press; 2002.

Encinas JM, Vaahtokari A, Enikolopov G. Fluoxetine targets early progenitor cells in the adult brain. Proc Natl Acad Sci USA 2006;103:8233–8238. [PubMed: 16702546]

Freund TF, Buzsáki G. Interneurons of the hippocampus. Hippocampus 1996;6:347–470. [PubMed: 8915675]

Freund TF, Ylinen A, Miettinen R, Pitkänen A, Lahtinen H, Baimbridge KG, Riekkinen PJ. Pattern of neuronal death in the rat hippocampus after status epilepticus. Relationship to calcium binding protein content and ischemic vulnerability. Brain Res Bull 1992;28:27–38. [PubMed: 1347249]

Gilbert P, Kesner R, Lee I. Dissociating hippocampal subregions: A double dissociation between dentate gyrus and CA1. Hippocampus 2001;11:626–636. [PubMed: 11811656]

Gluck, MA.; Myers, CE. Gateway to Memory: An Introduction to Neural Network Modeling of the Hippocampus in Learning and Memory. Cambridge, MA: MIT Press; 2001.

Gulyás AI, Acsády L, Freund TF. Structural basis of the cholinergic and serotonergic modulation of GABAergic neurons in the hippocampus. Neurochem Int 1999;34:359–372. [PubMed: 10397363]

Halasy K, Somogyi P. Subdivisions in the multiple GABAergic innervation of granule cells in the dentate gyrus of the rat hippocampus. Eur J Neurosci 1993;5:411–429. [PubMed: 8261118]

Hampson R, Deadwyler S. Information processing in the dentate gyrus. Epilepsy Res Suppl 1992;7:291–299. [PubMed: 1466769]

Harley CW. Norepinephrine and the dentate gyrus. Prog Brain Res 2007;163:299–318. [PubMed: 17765726]

Henze DA, Wittner L, Buzsáki G. Single granule cells reliably discharge targets in the hippocampal CA3 network *in vivo*. Nat Neurosci 2002;5:790–795. [PubMed: 12118256]

Houser CR. Interneurons of the dentate gyrus: An overview of cell types, terminal fields and neurochemical identity. Prog Brain Res 2007;163:217–232. [PubMed: 17765721]

Hunsaker MR, Rosenberg JS, Kesner RP. The role of the dentate gyrus, CA3a,b, and CA3c for detecting spatial and environmental novelty. Hippocampus 2008;18:1064–1073. [PubMed: 18651615]

Jackson MB, Scharfman HE. Positive feedback from hilar mossy cells to granule cells in the dentate gyrus revealed by voltage-sensitive dye and microelectrode recording. J Neurophysiol 1996;76:601–616. [PubMed: 8836247]

Jaffe DB, Gutiérrez R. Mossy fiber synaptic transmission: Communication from the dentate gyrus to area CA3. Prog Brain Res 2007;163:109–132. [PubMed: 17765714]

Kempermann, G. Adult Neurogenesis. Oxford, UK: Oxford University Press; 2006.

Kesner RP. A behavioral analysis of dentate gyrus function. Prog Brain Res 2007;163:567–576. [PubMed: 17765738]

Leranth C, Hajszan T. Extrinsic afferent systems to the dentate gyrus. Prog Brain Res 2007;163:63–84. [PubMed: 17765712]

Leranth C, Nitsch R, Deller T, Frotscher M. Synaptic connections of seizure-sensitive neurons in the dentate gyrus. Epilepsy Res Suppl 1992;7:49–64. [PubMed: 1361332]

Leutgeb JK, Leutgeb S, Moser M-B, Moser EI. Pattern separation in the dentate gyrus and CA3 of the hippocampus. Science 2007;315:961–966. [PubMed: 17303747]

Levy W. An information/computation theory of hippocampal function. Abstr Soc Neurosci 1985;11:493.

Levy, W. Hippocampal theories and the information/computation perspective. In: Erinoff, L., editor. NIDA Monographs: Neurobiology of Drug Abuse: Learning and Memory. Rockville, MD: US Department of Health and Human Services, National Institute on Drug Abuse; 1990. p. 116-125.

Levy, W.; Desmond, N. Synaptic Modification, Neuron Selectivity, and Nervous System Organization. Levy, W.; Anderson, J.; Lehmkuhle, S., editors. Hillsdale, NJ: Lawrence Erlbaum Associates; 1985. p. 110-123.

Lisman JE. Relating hippocampal circuitry to function: Recall of memory sequences by reciprocal dentate-CA3 interactions. Neuron 1999;22:233–242. [PubMed: 10069330]

Lisman JE, Otmakhova NA. Storage, recall, and novelty detection of sequences by the hippocampus: Elaborating on the SOCRATIC model to account for normal and aberrant effects of dopamine. Hippocampus 2001;11:551–568. [PubMed: 11732708]

Lisman JE, Talamini L, Raffone A. Recall of memory sequences by interaction of the dentate and CA3: A revised model of the phase procession. Neural Netw 2005;18:1191–1201. [PubMed: 16233972]

Lörincz A, Buzsáki G. Two-phase computational model training long-term memories in the entorhinal-hippocampal region. Ann N Y Acad Sci 2000;911:83–111. [PubMed: 10911869]

Marr D. Simple memory: A theory for archicortex. Proc R Soc Lond B Biol Sci 1971;262:23–81.

McClelland JL, Goddard NH. Considerations arising from a complementary learning systems perspective on hippocampus and neocortex. Hippocampus 1996;6:654–665. [PubMed: 9034852]

McNaughton BL. Associative pattern completion in hippocampal circuits: New evidence and new questions. Brain Res Brain Res Rev 1991;16:202–204.

McNaughton BL, Morris R. Hippocampal synaptic enhancement and information storage. Trends Neurosci 1987;10:408–415.

McNaughton, BL.; Barnes, CA.; Mizomori, SY.; Green, EJ.; Sharp, PE. The contribution of granule cells to spatial representation in hippocampal circuits: A puzzle. In: Morrell, F., editor. Kindling and Synaptic Plasticity: The Legacy of Graham Goddard. Boston: Springer-Verlag; 1991. p. 110-123.

Meeter M, Talamini L, Murre J. Mode shifting between storage and recall based on novelty detection in oscillating hippocampal circuits. Hippocampus 2004;14:722–741. [PubMed: 15318331]

Milner TA, Bacon CE. Ultrastructural localization of somatostatin-like immunoreactivity in the rat dentate gyrus. J Comp Neurol 1989;290:544–560. [PubMed: 2613944]

Milner TA, Veznedaroglu E. Ultrastructural localization of neuropeptide Y-like immunoreactivity in the rat hippocampal formation. Hippocampus 1992;2:107–125. [PubMed: 1308177]

Morgan RJ, Soltesz I. Nonrandom connectivity of the epileptic dentate gyrus predicts a major role for neuronal hubs in seizures. Proc Natl Acad Sci USA 2008;105:6179–6184. [PubMed: 18375756]

Morgan RJ, Santhakumar V, Soletsz I. Modeling the dentate gyrus. Prog Brain Res 2007;163:639–658. [PubMed: 17765743]

Myers CE, Ermita B, Harris K, Hasselmo M, Solomon P, Gluck M. A computational model of the effects of septohippocampal disruption on classical eyeblink conditioning. Neurobiol Learn Mem 1996;66:51–66. [PubMed: 8661251]

Myers CE, Ermita B, Hasselmo M, Gluck M. Further implications of a computational model of septohippocampal cholinergic modulation in eyeblink conditioning. Psychobiology 1998;26:1–20.

Norman KA, O'Reilly RC. Modeling hippocampal and neocortical contributions to recognition memory: A complementary-learning-systems approach. Psych Rev 2003;110:611–646.

O'Reilly R, McClelland J. Hippocampal conjunctive encoding, storage, and recall: Avoiding a tradeoff. Hippocampus 1994;4:661–682. [PubMed: 7704110]

Otis TS, Staley KJ, Mody I. Perpetual inhibitory activity in mammalian brain slices generated by spontaneous GABA release. Brain Res 1991;545:142–150. [PubMed: 1650273]

Patton P, McNaughton B. Connection matrix of the hippocampal formation. I. The dentate gyrus. Hippocampus 1995;5:245–286. [PubMed: 8589792]

Radley JJ, Jacobs BL. 5-HT1A receptor antagonist administration decreases cell proliferation in the dentate gyrus. Brain Res 2002;955:264–267. [PubMed: 12419546]

Rapp P, Gallagher M. Preserved neuron number in the hippocampus of aged rats with spatial learning deficits. Proc Natl Acad Sci USA 1996;93:9926–9930. [PubMed: 8790433]

Ratzliff A, Howard AL, Santhakumar V, Osapay I, Soletsz I. Rapid deletion of mossy cells does not result in a hyperexcitable dentate gyrus: Implications for epileptogenesis. J Neurosci 2004;24:2259–2269. [PubMed: 14999076]

Rokers B, Myers CE, Gluck M. A dynamic model of learning in the septo-hippocampal system. Neurocomputing 2000;32:501–507.

Rolls, ET. Function of neuronal networks in the hippocampus and neocortex in memory. In: Byrne, J.; Berry, W., editors. Neural Models of Plasticity: Experimental and Theoretical Approaches. San Diego: Academic Press; 1989a. p. 240-265.

Rolls, ET. Functions of neuronal networks in the hippocampus and cerebral cortex in memory. In: Cotterill, R., editor. Models of Brain Function. New York: Cambridge University Press; 1989b. p. 15-33.

Rolls ET. A theory of hippocampal function in memory. Hippocampus 1996;6:601–620. [PubMed: 9034849]

Rolls ET. An attractor network in the hippocampus: Theory and neurophysiology. Learn Mem 2007;14:714–731. [PubMed: 18007016]

Rolls ET, Kesner RP. A computational theory of hippocampal function, and empirical tests of the theory. Prog Neurobiol 2006;79:1–48. [PubMed: 16781044]

Rolls ET, Stringer SM, Elliot T. Entorhinal cortex grid cells can map to hippocampal place cells by competitive learning. Network 2006;17:447–465. [PubMed: 17162463]

Santhakumar V, Aradi I, Soltesz I. Role of mossy fiber sprouting and mossy cell loss in hyperexcitability: A network model of the dentate gyrus incorporating cell types and axonal topography. J Neurophysiol 2005;93:437–453. [PubMed: 15342722]

Scharfman HE. Dentate hilar cells with dendrites in the molecular layer have lower thresholds for synaptic activation by perforant path than granule cells. J Neurosci 1991;11:1660–1673. [PubMed: 2045880]

Scharfman, HE. Differentiation of rat dentate neurons by morphology and electrophysiology in hippocampal slices: Granule cells, spiny hilar cells and aspiny, “fast-spiking” cells. In: Ribak, CE.; Gall, C.; Mody, I., editors. The Dentate Gyrus and Its Role in Seizures. New York: Elsevier; 1992. p. 93-109.

Scharfman HE. Electrophysiological evidence that hilar mossy cells are excitatory and innervate both granule cells and interneurons. J Neurophysiol 1995;74:179–194. [PubMed: 7472322]

Scharfman, HE. The role of nonprincipal cells in dentate gyrus excitability and its relevance to animal models of epilepsy and temporal lobe epilepsy. In: Delgado-Esqueta, AV.; Wilson, W.; Olsen, RW.; Porter, RJ., editors. Basic Mechanisms of the Epilepsies: Molecular and Cellular Approaches. Vol. 3rd ed.. New York: Lippincott-Raven; 1999. p. 805-820.

Scharfman, HE. The Dentate Gyrus: A Comprehensive Guide to Structure, Function, and Clinical Implications. New York: Elsevier; 2007a.

Scharfman HE. The CA3 “backprojection” to the dentate gyrus. Prog Brain Res 2007b;163:627–637. [PubMed: 17765742]

Scharfman HE, Schwartzkroin P. Electrophysiology of morphologically identified mossy cells of the dentate hilus recorded in guinea pig hippocampal slices. J Neurosci 1988;8:3812–3821. [PubMed: 2461436]

Scharfman HE, Schwartzkroin PA. Responses of cells of the fascia dentata to prolonged stimulation of the perforant path: Sensitivity of hilar cells and changes in granule cell excitability. Neuroscience 1990a;35:491–504. [PubMed: 2381513]

Scharfman HE, Schwartzkroin PA. Consequences of prolonged afferent stimulation of the rat fascia dentata: Epileptiform activity in area CA3 of hippocampus. Neuroscience 1990b;35:505–517. [PubMed: 2381514]

Scharfman HE, Kunkel DD, Schwartzkroin PA. Synaptic connections of dentate granule cells and hilar interneurons: Results of paired intracellular recordings and intracellular horseradish peroxidase injections. Neuroscience 1990;37:693–707. [PubMed: 2247219]

Seress L. Comparative anatomy of the hippocampal dentate gyrus in adult and developing humans. Prog Brain Res 2007;163:3–41. [PubMed: 17765709]

Sloviter RS, Zappone CA, Harvey BD, Bumanglag AV, Bender RA, Frotscher M. “Dormant basket cell” hypothesis revisited: Relative vulnerabilities of dentate gyrus mossy cells and inhibitory interneurons after hippocampal status epilepticus in the rat. J Comp Neurol 2003;459:44–76. [PubMed: 12629666]

Soriano E, Frotscher M. Mossy cells of the rat fascia dentata are glutamate-immunoreactive. Hippocampus 1994;4:65–69. [PubMed: 7914798]

Sperk G, Marksteiner J, Gruber B, Bellmann R, Mahata M, Ortler M. Functional changes in neuropeptide Y- and somatostatin-containing neurons induced by limbic seizures in the rat. Neuroscience 1992;50:831–846. [PubMed: 1360155]

Sperk G, Hamilton T, Colmers WF. Neuropeptides in the dentate gyrus. Prog Brain Res 2007;163:285–297. [PubMed: 17765725]

Squire L. Memory and the hippocampus: A synthesis from findings with rats, monkeys, and humans. Psychol Rev 1992;99:195–231. [PubMed: 1594723]

Treves A, Rolls E. Computational constraints suggest the need for two distinct input systems to the hippocampal CA3 network. Hippocampus 1992;2:189–200. [PubMed: 1308182]

Treves A, Rolls E. Computational analysis of the role of the hippocampus in memory. Hippocampus 1994;4:374–391. [PubMed: 7842058]

Treves A, Tashiro A, Witter ME, Moser EI. What is the mammalian dentate gyrus good for? Neuroscience 2008;154:1155–1172. [PubMed: 18554812]

Tsetsenis T, Ma XH, Lo Iacono L, Beck SG, Gross C. Suppression of conditioning to ambiguous cues by pharmacogenetic inhibition of the dentate gyrus. Nat Neurosci 2007;10:896–902. [PubMed: 17558402]

West MJ, Slomianka L, Gundersen HJ. Unbiased stereological estimation of the total number of neurons in the subdivisions of the rat hippocampus using the optical fractionator. Anat Rec 1991;231:482–497. [PubMed: 1793176]

Willshaw D, Buckingham J. An assessment of Marr's theory of the hippocampus as a temporary memory store. Philos Trans R Soc Lond B Biol Sci 1990;329:205–215. [PubMed: 1978365]

Wiskott L, Rasch M, Kempermann G. A functional hypothesis for adult hippocampal neurogenesis: Avoidance of catastrophic interference in the dentate gyrus. Hippocampus 2006;16:329–343. [PubMed: 16435309]

Yeckel MF, Berger TW. Feedforward excitation of the hippocampus by afferents from the entorhinal cortex: Redefinition of the role of the trisynaptic pathway. Proc Natl Acad Sci USA 1990;87:5832–5836. [PubMed: 2377621]

Zhao C, Deng W, Gage FH. Mechanisms and functional implications of adult neurogenesis. Cell 2008;132:645–660. [PubMed: 18295581]

Appendix

APPENDIX: SUMMARY OF SIMULTION DETAILS

Software was programmed in objective-C using the Xcode applications development suite for UNIX-based Macintosh OS 10.5.

The dentate gyrus network contains 500 simulated dentate granule cells, divided into 25 clusters or simulated laminae of 20 granule cells each. Each cluster contains one local interneuron, meant to simulate the effects of basket cells, axo-axonic cells, and other interneurons providing lateral surround feedback inhibition to granule cells. The network also contains 20 hilar mossy cells and 10 HIPP cells. External input to the network is provided by 100 simulated perforant path afferents. The output of the granule cells (mossy fibers) form the external output of the network.

To simulate the sparse connectivity in the dentate gyrus, perforant path afferents each contact a randomly determined 20% of granule cells and HIPP cells; mossy cells and HIPP cells each feedback to contact a randomly determined 20% of granule cells. Pilot simulations (not shown here) suggest that the network is relatively stable for fan-out probabilities in the range from 10 to 50%. Connections are initialized randomly at the start of each simulation run and fixed thereafter.

For simplicity, neurons update synchronously, during discrete trials. Each trial consists of one presentation of an input pattern, followed by each cell type computing its activation in response to that input pattern; the resulting granule cell outputs constitute the response of the network to that pattern. Except as otherwise noted, all results reported in the paper are averaged over five simulation runs.

Granule Cell Activity

For all granule cells j, activity y_j is calculated as a function of membrane potential V_j, $y_j = f(V_m)$. For simplicity, a linear identity function is used, clipped at $0 \leq y_j \leq 1$.

For each granule cell, membrane potential V_j is calculated as:

$$V_j = V_{\text{rest}}(j) + g_{e-pp}(j) - g_{i-\text{int}}(j) + g_{e-mc}(j) - g_{i-\text{HIPP}}(j) \quad \text{(A1)}$$

In Eq. (A1), $V_{rest}(j)$ is the resting potential of granule cell j, which is set to −0.30 as a default value in the simulations reported here. Figure A1A shows parametric manipulations in which simulations with various values of V_{rest} were trained on randomly constructed sets of 10 input patterns each with input density d = 10%. In general, pattern separation was relatively stable for a range of values of V_{rest} near 0.0. As V_{rest} grew high, too many granule cells became active even in the presence of weak entorhinal inputs, and pattern separation began to degrade. Conversely, as V_{rest} grew too small, very few granule cells would become active even in the presence of strong entorhinal afferents, and pattern separation again degraded.

Other variables in Eq. (A1) that contribute to membrane potential V_j include $g_{e-pp}(j)$, which is the net excitatory conductance from the perforant path afferents to j:

$$g_{e-pp}(j)=\sum_i y_i w_{ij} \tag{A2}$$

where y_i is the activity of the ith perforant path afferent ($0 \le y_i \le 1$) and w_{ij} is the strength of the synaptic connection between i and j. Perforant path to granule cell connections are weakly excitatory, initialized randomly from the uniform distribution U[0,1) at the start of each simulation run.

$g_{i-\text{int}}(j)$ is the net inhibitory conductance to j provided by GABAergic interneurons such as basket cells. For each granule cell j:

$$g_{i-\text{int}}(j)=\beta_{\text{INT}}\,\max_k(\forall_x y_x) \tag{A3}$$

where x are the granule cells in j's lamina, and $max_k()$ returns a value equal to the k^{th}-maximum; in the current simulations k is set to 1. β_{INT} is a constant governing the strength of lateral surround inhibition; in general, as β_{INT} increases, net inhibitory conductance increases, and most granule cells are silenced. For values of $\beta_{INT} \ge 1$, all granule cells are silenced. In the simulations reported here, β_{INT} is set to 0.9 as a default value. Figure A1B shows parametric manipulations in which simulations with various values of β_{INT} were trained on randomly constructed sets of 10 input patterns each with input density of d = 10% or d = 5%. For relatively dense input patterns (d = 10%), there is little effect of changing β_{INT}, except as β_{INT} approaches 1, at which point all granule cells are silenced by inhibition. However, for lower input density (d = 5%), average percent overlap is minimized—and pattern separation is strong—for values of β_{INT} near 0.9, which silence most granule cells in each cluster while leaving a few active.

$g_{e-mc}(j)$ and $g_{i-\text{HIPP}}(j)$ are conductances contributed by mossy cells and HIPP cells, respectively; these are discussed further below.

Excitatory Inputs From Hilar Mossy Cells (g_{e-mc})

Each hilar mossy cell m calculates its activity y_m as:

$$y_m=\sum_j y_j \tag{A4}$$

for all granule cells j from which it receives input. Mossy cells inputs are conditional; that is, they do not directly excite granule cells, but increase the activity of granule cells that are already responding to perforant path inputs. The basis for this conditional approach is the nature of mossy cell excitation of granule cells that was defined experimentally, using simultaneous

recordings from monosynaptically connected mossy cells and granule cells in hippocampal slices (Scharfman, 1995). When a presynaptic mossy cell was stimulated to discharge in response to injected current, the unitary EPSP in the postsynaptic granule cell was greater in amplitude if the granule cell was depolarized. At resting potential, the unitary EPSP of the granule cell was smaller. These data suggest that the excitation of granule cells by mossy cells is maximal when a granule cell is already depolarized.

For each granule cell *j*, the effect of mossy cells is computed as:

$$g_{e-mc}=\beta_{\mathrm{MC}}\sum_{m}y_m w_{mj} \tag{A5}$$

where w_{mj} = 1 for those mossy cells m providing input to *j*, and 0 otherwise. Note that g_{e-mc} serves to increase the activity of those granule cells that have survived local inhibition ("rich-get-richer"). In the current simulations, β_{MC} = 5.0 except as otherwise noted; Figure 7 explored parametric manipulations with β_{MC}, showing that pattern separation is relatively stable unless β_{MC} grows very small, at which point few granule cells receive enough feedback excitation from mossy cells to remain active.

Inhibitory Inputs From Hilar Interneurons ($g_{i-\mathrm{HIPP}}$)

Each HIPP cell *h* calculates its activity y_h as:

$$y_h=\sum_{i}w_{ih}y_i \tag{A6}$$

for all perforant afferents *i*, where w_{ih} = 1 for those perforant path afferents providing input to *h*, and 0 otherwise. Each HIPP provides feedforward inhibition to those granule cells it contacts and that have not yet been silenced by feedback inhibition:

$$g_{i-\mathrm{HIPP}}=\beta_{\mathrm{HIPP}}\sum_{h}y_h w_{hj} \tag{A7}$$

where w_{hj} = 1 for those granule cells *j* receiving input from *h* and 0 otherwise. Note that $g_{i-\mathrm{HIPP}}$ increases linearly with density of entorhinal input activity, and therefore provides a normalizing effect on granule cell output for densely active entorhinal input patterns. In the current simulations, β_{HIPP} = 0.1, except as otherwise noted; Figure 7 explored parametric manipulations with β_{HIPP}, showing that pattern separation is relatively stable unless β_{HIPP} grows very large, at which point most granule cells are silenced by inhibition from HIPP cells.

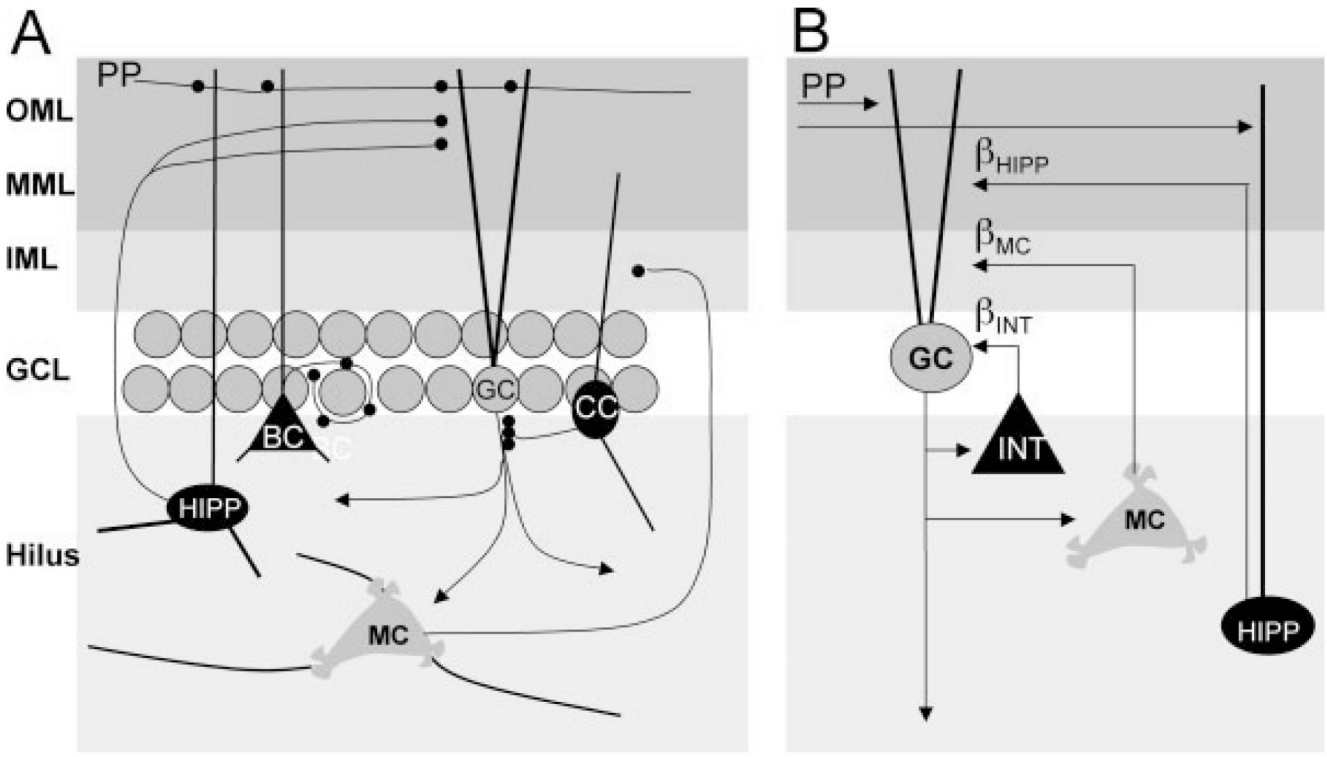

FIGURE 1.

(A) Schematic of some major cell types and connections in the dentate gyrus. Granule cell (GC) bodies lie in the granule cell layer (GCL), with dendrites extending through the inner molecular layer (IML), middle molecular layer (MML), and outer molecular layer (OML), where they receive afferents from the entorhinal cortex layer II neurons via the perforant path (PP). GC axons form the mossy fibers, which synapse in area CA3 (not shown) and also ramify widely within the hilus, synapsing on cell types including the mossy cells (MC), which project primarily to the inner molecular layer, and hilar interneurons. One subtype of hilar interneuron that is prominent in the model is the HIPP cell, which has a hilar cell body and axon that projects primarily to the outer two-thirds of the molecular layer, the location where the perforant path terminates. HIPP cell dendrites extend into the molecular layer, where they are targeted by the PP. Other GABAergic cell types include basket cells (BC), which project to GC bodies, and chandelier cells (CC), which target the axon initial segment of GCs. (B) Elements incorporated in the computational model include GCs, which receive input from the PP and whose axons provide the principal output of the network; interneurons (INT) that innervate GCs; MCs, which are excited by GCs and provide widely ramifying feedback to GCs across the network; and HIPP cells, which receive PP input and inhibit GCs. The global influence of INT, hilar MCs, and HIPP cells on GCs is specified in the model by three constants, β_{INT}, β_{MC}, and β_{HIPP}, which can be modified to simulate upregulation or downregulation of the effect of each cell type on GC activity.

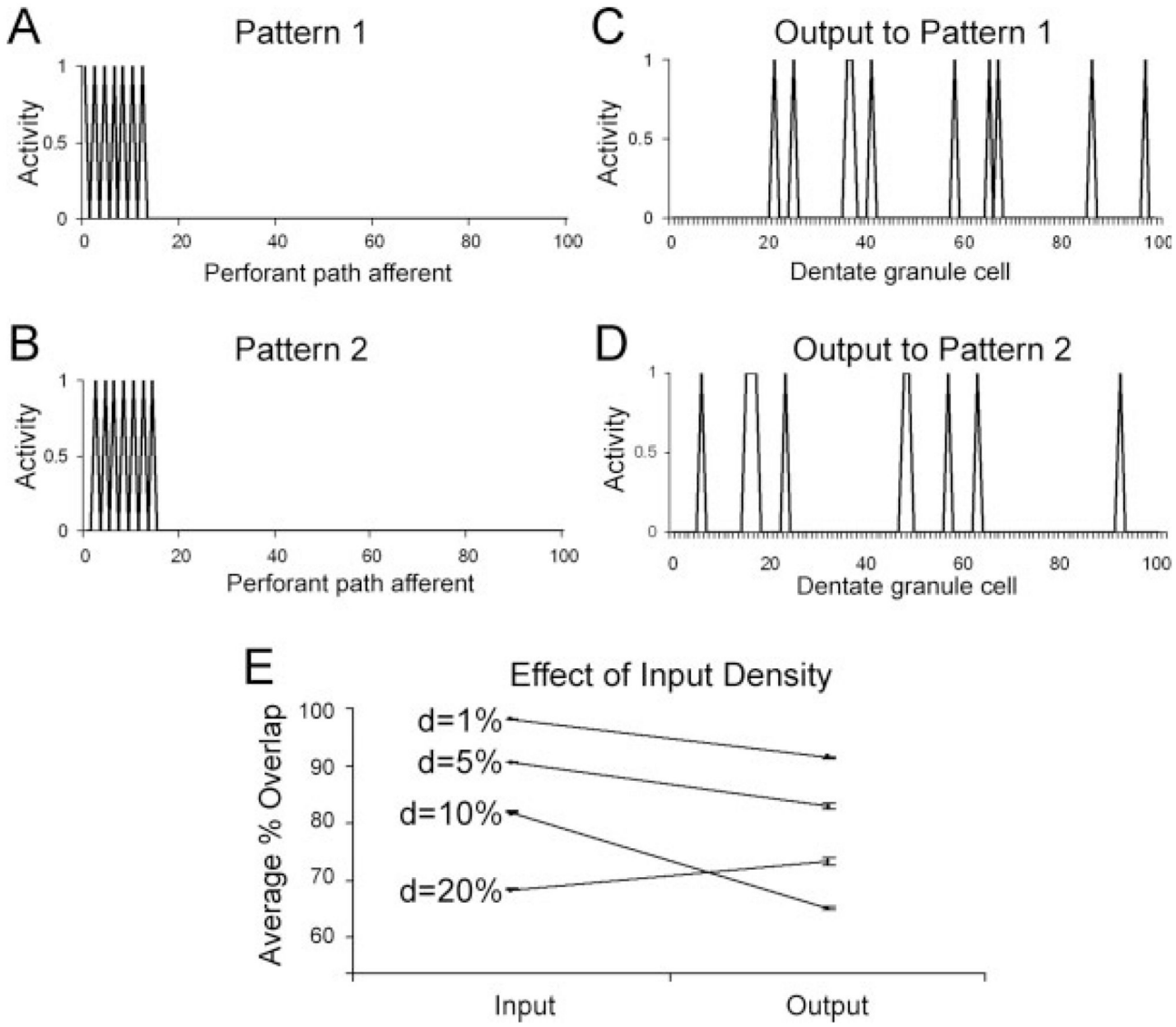

FIGURE 2.

Example of input and output patterns in the dentate gyrus model. (A) and (B) show two input patterns, presented as activity along the 100 perforant path afferents. Each pattern has seven active perforant path afferents, six of which are common between the two patterns; hence the two patterns are highly overlapping. (C) and (D) show the output, as granule cell activity, to each input pattern in a sample simulation run. For clarity, only the first 100 granule cells are shown; these 100 cells were representative of the larger sample of 500 granule cells in the model. In both (C) and (D), a similar percentage of granule cells become active, but the particular granule cells responding to each pattern differ. Thus, there is less overlap in the outputs than was initially present in the inputs—and so pattern separation has occurred. (E) Results of the model, trained on sets of 10 randomly constructed input patterns, for various densities *d* of perforant path activation. Pattern separation occurs if the overlap, measured at the granule cell outputs, is less than the overlap measured at the inputs. For low-to-moderate input density ($d \leq 10\%$), average percent overlap computed at the granule cell outputs is higher than the overlap of the inputs—meaning that pattern separation has occurred. For denser input

patterns (d = 20%), the percent overlap measured at the outputs is actually higher than that of the inputs—meaning that pattern separation has failed.

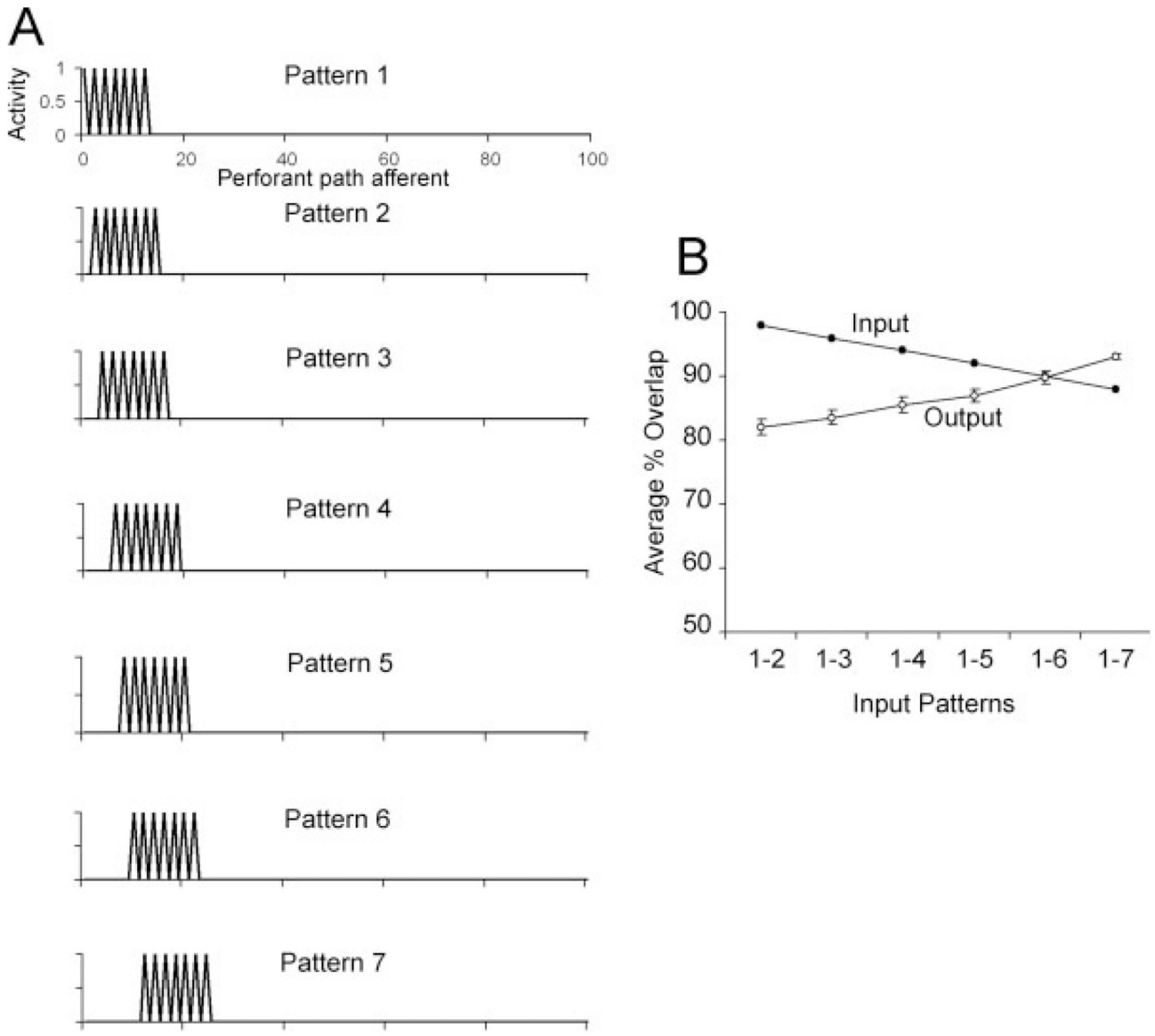

FIGURE 3.

Simulation of the Leutgeb et al. (2007) "morphed environments." (A) To simulate the "morphed environments," a set of overlapping input patterns was constructed. These patterns are then presented, one at a time, as inputs to the dentate gyrus model. (B) Average percent overlap for the input patterns shown in A was highest for "neighboring" patterns such as Patterns 1 and 2, and progressively less for more distinct pairs of patterns such as the extreme Patterns 1 and 7. Average percent overlap, computed across granule cell outputs in the model, was strongly decreased for the most overlapping inputs (e.g., Patterns 1 and 2 or Patterns 1 and 3), but there was less decrease for patterns that were already fairly distinct—and actually a slight increase in overlap for the extremely different input Patterns 1 and 7. Thus, pattern separation in the model is greatest for inputs that overlap extensively.

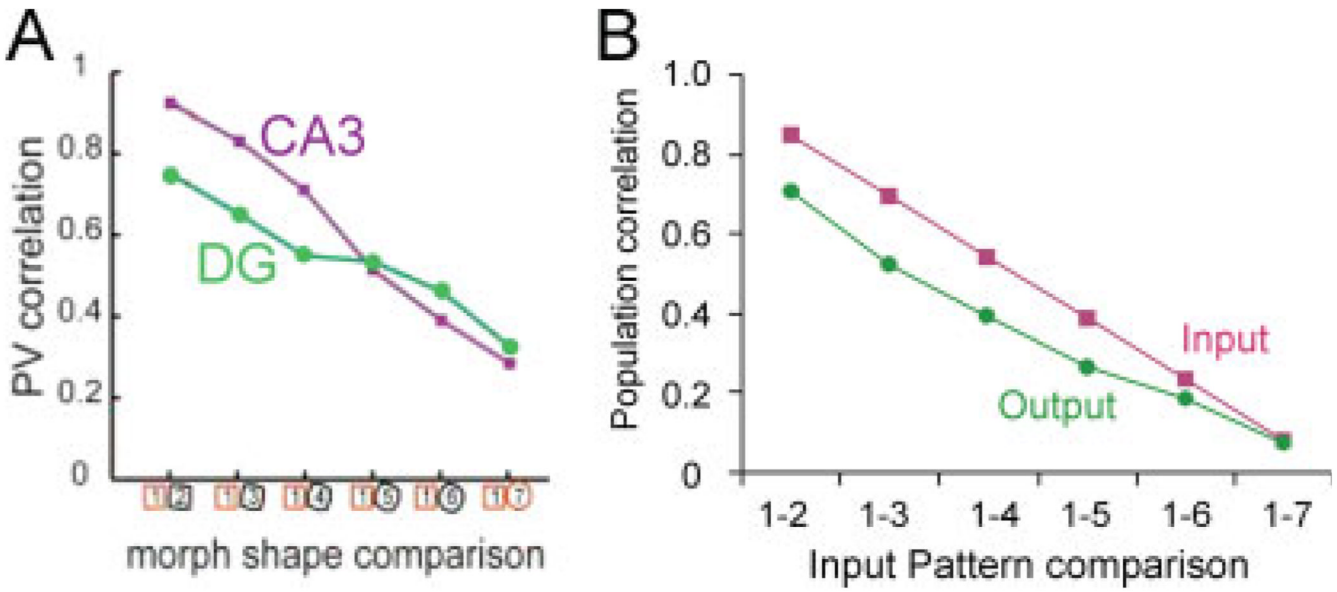

FIGURE 4.

(A) In rats, population responses in CA3 are highly correlated in neighboring environments, and this correlation decreases approximately linearly as environmental difference increases; in contrast, there is less correlation in dentate gyrus (DG) responses, particularly for environments that are very similar. Adapted from Leutgeb et al. (2007), Figure 2C. (B) Population responses from dentate granule cells in the model ("Output") also show reduced correlation for neighboring stimuli, compared with correlations that exist in the input patterns ("Input"). [Color figure can be viewed in the online issue which is available at www.interscience.wiley.com.]

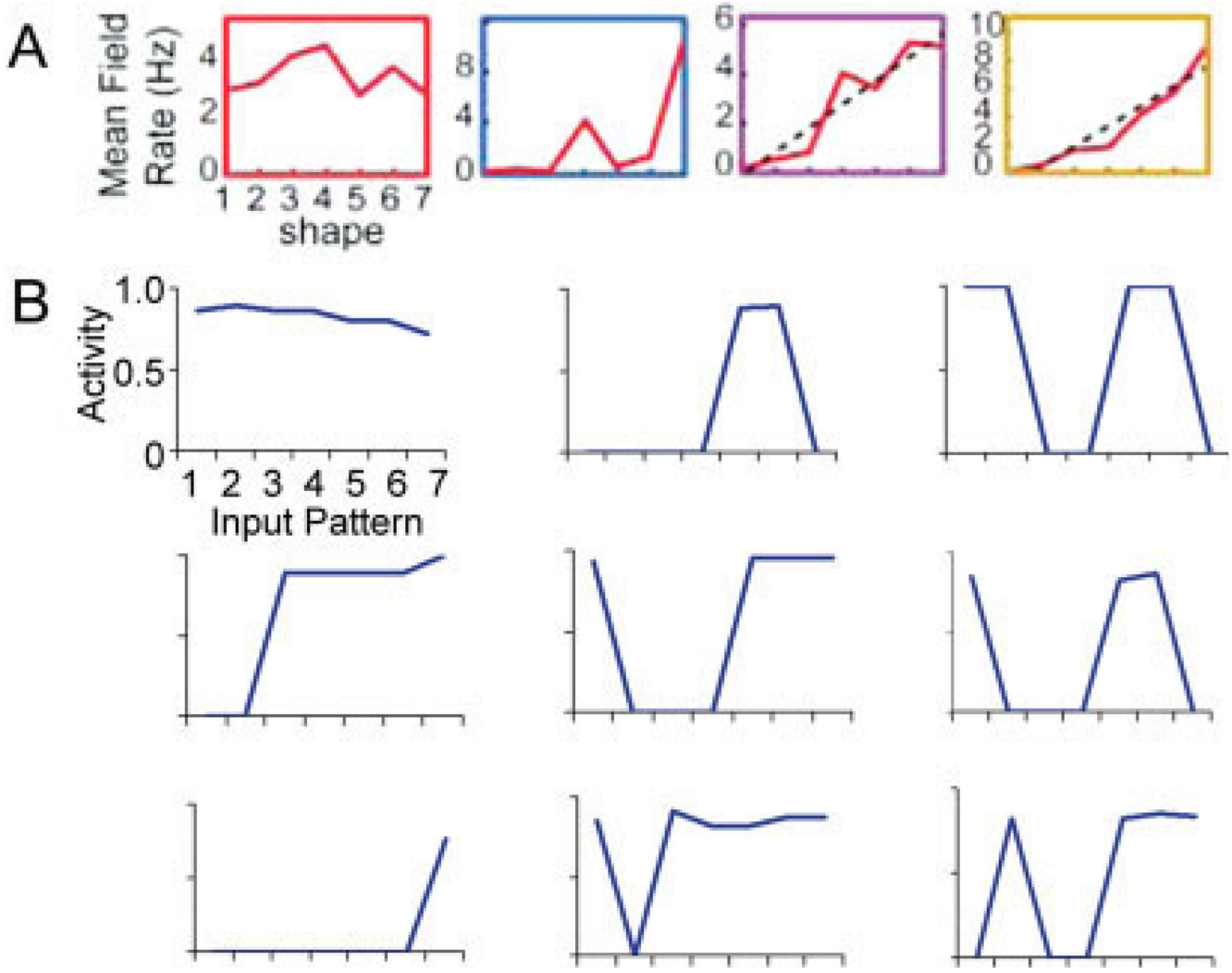

FIGURE 5.

(A) Mean responses from representative dentate granule cells in rats as the environment is progressively "morphed" through seven stages; response curves can be linear, sigmoidal, and even biphasic. Adapted from Leutgeb et al. (2007; Fig. 2C). (B) Individual granule cells in the model show a similar phenomenon. Some cells (top left) respond in a weakly linear or monotonic fashion across the set of patterns; others (center left, bottom left) respond or fail to respond to a set of adjoining patterns; still others (center, right) have biphasic response curves, responding selectively to more than one nonadjacent pattern. [Color figure can be viewed in the online issue which is available at www.interscience.wiley.com.]

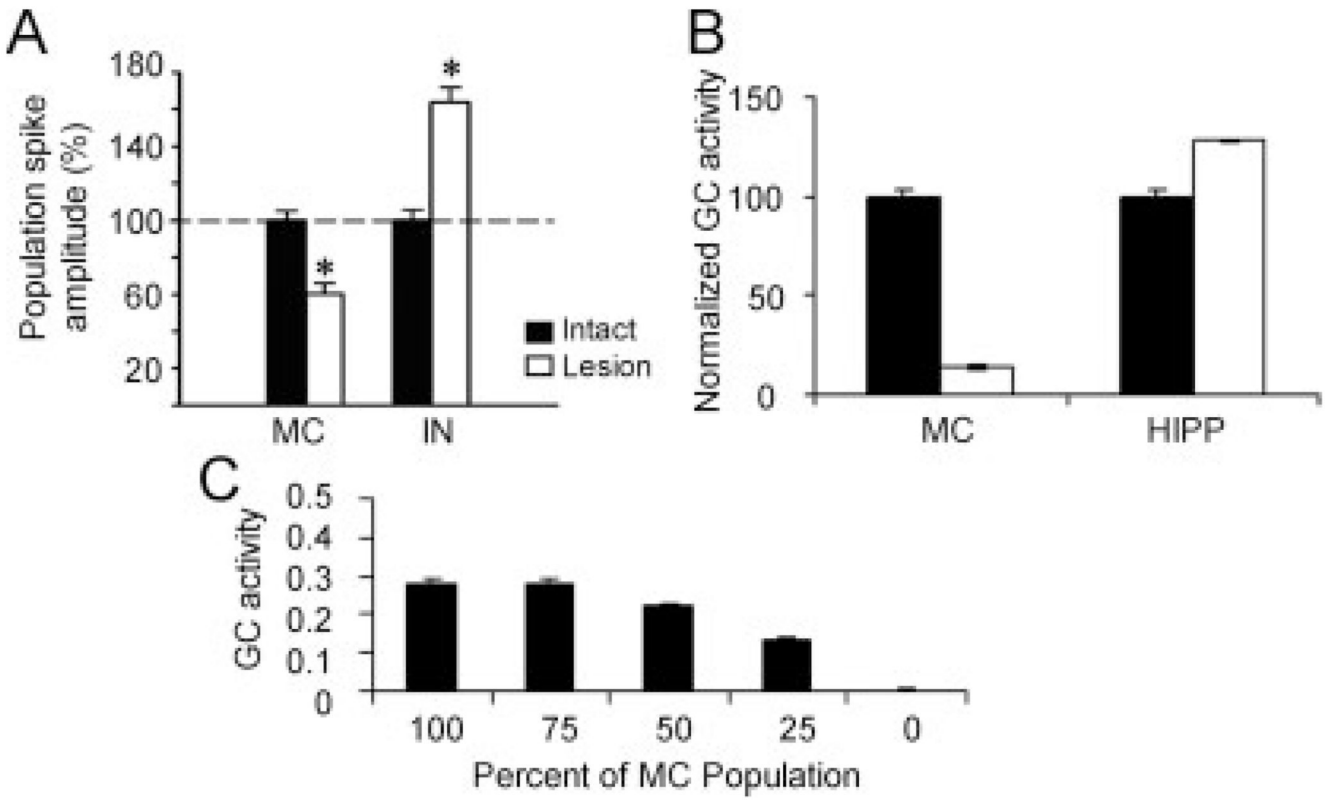

FIGURE 6.

(A) Recordings from the granule cell layer suggest that the field potential evoked by perforant path stimulation, reflecting granule cell activation, decreases following ablation of a subset of mossy cells (MC), and increases following hilar interneuron (IN) ablation. Adapted from Ratzliff et al. (2004; Fig. 3F). (B) In the model, granule cell activation by the perforant path is similarly influenced by ablating MCs or HIPP cells. (C) In the model, granule cell (GC) activation by the perforant path declines as increasing percentages of mossy cells are deleted.

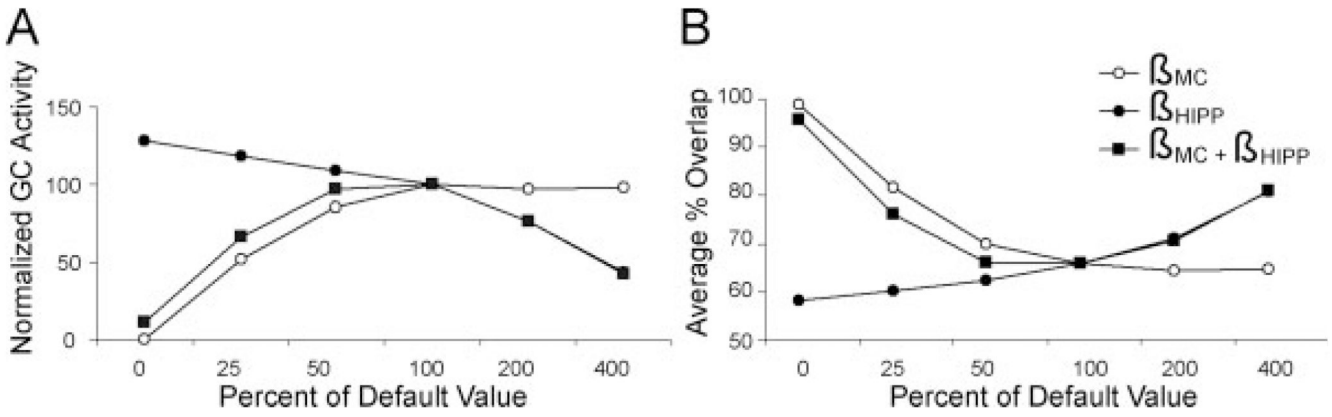

FIGURE 7.

In the model, hilar function can be upregulated and downregulated by changing the free parameters β_{MC} and β_{HIPP} that regulate the effect of mossy cells and HIPP cells on granule cell activity. In general, both (A) granule cell (GC) activity, and (B) pattern separation (measured as reduction in percent overlap at the granule cell outputs), decrease as β_{MC} is reduced from its "default" value of 5.0–50% or less of that default value; in contrast, both granule cell activity and pattern separation tend to increase as β_{HIPP} is increased from its "default" value of 0.1–200% or greater of that default value. These default values were chosen in the model because they approximately optimize pattern separation. Granule cell activity in (A) is plotted as percentage of activity at "default" parameter values.

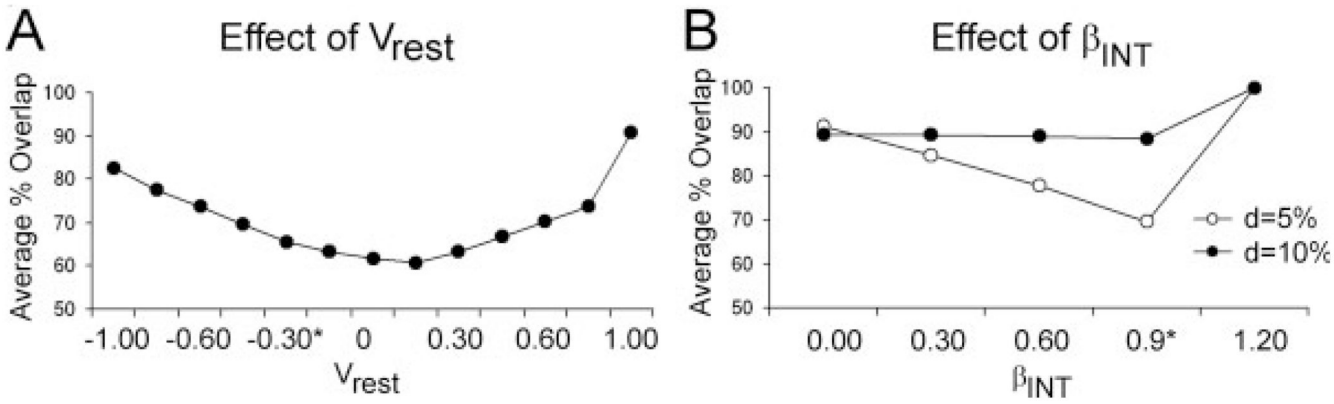

FIGURE A1.

Parametric manipulations of the granule cell resting potential V_{rest} and GABAergic inhibition to granule cells, β_{INT}, in the model. (A) Pattern separation is relatively stable for a range of values of V_{rest} near 0.0, but begins to degrade as V_{rest} increases or decreases. (B) For patterns of moderate density (d = 10%), pattern separation is relatively stable for a range of values of β_{INT}, except as β_{INT} approaches or exceeds 1.0, at which point all granule cells are silenced by inhibition. For input patterns of sparser density (d = 5%), average percent overlap is minimized—and pattern separation is strong—for values of β_{INT} near 0.9, which silence most (but not all) granule cells.

TABLE 1

Key Parameters Governing Pattern Separation Behavior in the Dentate Gyrus Model

Parameter	Description	Default value
V_{rest}	Resting potential of granule cells—defines the initial "bias" of granule cells to spontaneously discharge	−0.30
β_{INT}	Interneuron constant—affects the global strength of lateral surround feedback inhibition on granule cells	0.9
β_{HIPP}	HIPP cell constant—affects the global strength of HIPP inhibition on granule cells	0.1
β_{MC}	Mossy cell constant—affects the global strength of mossy cells to facilitate granule cell firing	5.0